(11/28/09 draft by GLP for JANNAF 43rd CS, Dec. 7-11, 2009)

Nitric Oxide and Oxygen Air-Contamination Effects on Extinction Limits of Non-premixed Hydrocarbon-Air Flames for a HIFiRE Scramjet

Gerald L. Pellett*, Lucy C. Dawson[2], Sarah N. Vaden[3], and Lloyd G. Wilson[4]

NASA Langley Research Center, Hampton, VA 23681

ABSTRACT

Unique nitric oxide (NO) and oxygen air-contamination effects on the extinction Flame Strength (FS) of non-premixed hydrocarbon (HC) vs. "air" flames are characterized for 7 gaseous HCs, using a new idealized 9.3 mm straight-tube Opposed Jet Burner (OJB) at 1 atm. FS represents a laminar strain-induced extinction limit based on cross-section-average air jet velocity, U_{air}, that sustains combustion of a counter jet of gaseous fuel just before extinction. Besides ethane, propane, butane, and propylene, the HCs include ethylene, methane, and a 64 mole-% ethylene / 36 % methane mixture, the writer's previously recommended gaseous surrogate fuel for HIFiRE scramjet tests. The HC vs. clean air part of the work is an extension of a May 2008 JANNAF paper that characterized surrogates for the HIFiRE project that should mimic the flameholding of reformed (thermally- or catalytically-cracked) endothermic JP-like fuels. The new FS data for 7 HCs vs. clean air are thus consolidated with the previously validated data, normalized to absolute (local) axial-input strain rates, and co-plotted on a dual kinetically dominated reactivity scale. Excellent agreement with the prior data is obtained for all 7 fuels. Detailed comparisons are also made with recently published (Univ. Va) numerical results for ethylene extinction. A 2009-revised ethylene kinetic model (Univ. Southern Cal) led to predicted limits within ~ 5 % (compared to 45 %, earlier) of this writer's 2008 (and present) ethylene FSs, and also with recent independent data (Univ. Va) obtained on a new OJB system. These $\pm$ 5 % agreements, and a hoped-for "near-identically-performing" reduced kinetics model, would greatly enhance the capability for accurate numerical simulations of surrogate HC flameholding in scramjets.

The measured air-contamination effects on normalized FS extinction limits are projected to assess ongoing Arc-Heater-induced "facility test effects" of NO production (e.g., 3 mole-%) and resultant oxygen depletion (from 21 to 19.5 %), for testing the "64/36" surrogate fuel in Langley's Arc-Heated Scramjet Test Facility for HIFiRE engine designs. The FS results show a generally small ($\leq$ 4 %) "nitric oxide enhancement" effect, relative to clean air, for up to 3 % NO (free-stream Mach number up to 7 in Arc Jet testing). However, a progressively large "oxygen-deficiency weakening" effect develops. For 3 % NO, a net weakening of 26 % in FS is derived for the "64/36" fuel vs. air. The corresponding net weakening for pure ethylene is 20 %. A number of practical recommendations regarding facility test effects are offered.

---

* Senior Research Scientist, Hypersonic Air Breathing Propulsion Branch, Research and Technology Directorate. MS 168, NASA Langley Research Center, Hampton, VA 23681. g.l.pellett@larc.nasa.gov

[2] NASA-Langley Virginia Governor's School Participant, summer 2009. Senior at: Loudoun Valley HS, Purcellville, VA; and Loudoun County Academy of Science, Sterling, VA.

[3] NASA-Langley Virginia Governor's School Participant, summer 2006; and LARSS student, summers of 2007 and 2008. Student at Georgia Tech since July 2008.

[4] Senior Technician, Lockheed Martin Space Operations, Hampton, VA

INTRODUCTION

Early NASA Langley attempts to realize the high-speed potential of (airbreathing) Supersonic Combustion Ramjet (SCRAMJET) propulsion used gaseous hydrogen fuel, and resulted in two successful flight demonstrations (Hyper-X). However, recent interest has focused on the use of vaporized endothermic hydrocarbon (HC) fuels. Unfortunately, vaporized liquid HCs have been of limited use in hoped-for scramjet applications, because they *are far less reactive*, even though they are obviously much easier to store and handle. And although endothermic catalytic cracking of HCs has been investigated to improve both reactivity and cooling capacity [1-6], very significant problems remain. A simplified bypass approach is to decouple endothermic cracking requirements from scramjet combustion processes, by using reactive gaseous surrogate HC fuels in scramjet combustors, as in ongoing HIFiRE[1] tests being conducted in NASA Langley's Arc-Heated Scramjet Test Facility (AHSTF), where arc-heated air is diluted with clean dry air just before expansion through a facility nozzle.

Although operation of the Arc-Heated facility avoids certain problems associated with combustion-heated facilities that produce substantial steam and carbon dioxide air contaminants, relatively small amounts of nitric oxide (NO), and typically require oxygen make-up, the Arc-Heater does produce significant NO with a corresponding reduction in O_2 and N_2, as discussed later in a review of facility test effects on scramjet ignition and flameholding processes.

As might be expected, difficult and competing performance challenges remain to achieve ignition and robust flameholding-combustion with various multi-component liquid fuels, and even their gaseous surrogates, injected just upstream of relatively small subsonic cavity flameholders and also directly within [4-25]. Some important goals are to (1) promote rapid initial reaction, with sufficient production and transport of radicals and (usually limited) enthalpy to the overriding supersonic shear layer, (2) avoid excessive internal drag and loss of net thrust, or much worse, loss of flameholding, and (3) achieve needed "endothermic" heat soak and enhanced fuel reactivity in active cooling channels *without* the formation and deposition of significant carbon residues [3-6]. Thus thermally- or (more likely) catalytically-cracked fuel vapor and entrained air must mix, diffuse and react long enough in a subsonic cavity recirculation zone to achieve robust "incipient flameholding" (after auto- or spark-induced-ignition), to supply adequate radicals and enthalpy to the mainstream supersonic flow with minimal loss of kinetic energy.

Opposed Jet Burner (OJB) tools have been used extensively in past studies by the authors to measure the quasi-steady extinction limits of various laminar non-premixed, pure and N_2-diluted fuel vs. air Counterflow Diffusion Flames (CFDFs) at one atmosphere [26-38]. Early efforts focused on: (1) The velocity [36] and thermal structure [28,35], and strain-induced extinction of 14 to 100 % hydrogen–air CFDFs, summarized in Ref. 26; (2) the efficacy of silane/hydrogen (and silane/HC) mixtures for promoting ignition and piloting (without extinction) of very high speed combustion [27,33], including that used in the Hyper-X; and (3) the effects of test facility contaminants in vitiated air on H_2–air extinction limits [29-32,34]. The latter test effects were reviewed and used to assess possible differences in "incipient flameholding," compared to clean air in flight, in the subsonic re-circulating cavity flows of an otherwise supersonic combustor [39,40]. The CFDF studies showed that Flame Strength, FS, defined locally as the laminar maximum cross-section-average air input velocity, U_{air}, that sustains combustion of a counterflowing jet of gaseous fuel just before extinction,

[1] The Hypersonic International Flight Research and Experimentation (HIFiRE) program is a bi-lateral collaboration executed by an integrated team representing the U.S. Air Force Research Laboratory (AFRL) and the Australian Defence Science and Technology Organisation (DSTO). Further, the US Air Force has secured a Space Act Agreement with NASA to advance the collaborative development and demonstration of hypersonic aeropropulsion technologies. The objective of the HIFiRE program is to increase understanding of fundamental hypersonic phenomena and to develop technologies deemed critical to the realization of next generation aerospace vehicles. The purpose is to extend the hypersonic database and enhance the accuracy of complex models and simulations. Phenomena will be examined and characterized at flight conditions that are difficult, if not impossible, to model with current computational methods and/or simulate in ground test facilities. The product of this program is an experimental flight laboratory to capture extensive coherent high-fidelity data. The scope of this program encompasses a series of 8 focused research projects. For further information see Ref. [83].

represents an important combustion parameter. FS uniquely characterizes a kinetically dominated fuel combustion rate that is nevertheless influenced by diffusion effects, including the diffusion of pure fuel from the stagnation point. More generally, Applied Stress Rates (ASRs) at extinction (U_{air} normalized by nozzle or tube diameter, $D_{n\ or\ t}$) can be compared directly with extinction limits determined numerically using either a 1-D or (preferably) a 2-D Navier Stokes simulation with detailed transport and finite rate chemistry. Thus our early studies concluded that (1) FS limits should effectively scale with hypothetical "idealized" scramjet flameholding limits [26,39,40], and (2) measured global Applied Stress Rates at extinction for either convergent-nozzle-OJBs (ASR_n) or straight-tube-OJBs (ASR_t) can be compared quantitatively with numerically simulated laminar extinction limits [26,35-37,41]. Such limits may be evaluated with reasonable accuracy using either a 1-D Navier Stokes stream-function approximation [see 26,37] with detailed transport and finite rate chemistry, or better yet, a fully detailed 2-D Navier Stokes numerical simulation [41] that has greater fidelity when applied to finite nozzles and tubes with prescribed inflow profiles.

In a 2007 paper [45], which followed [44] and earlier work [42,43], we conducted a logical progression of experimental and analytic studies that helped define the combustion and extinction of gaseous HC–air CFDFs. Whereas [44] included FS results for six single-component hydrocarbon (HC) fuels (always pure, and sometimes nitrogen-diluted), and also three HC-diluted H_2 fuels that showed very nonlinear decays in FS as HC was added, [45] was the first to characterize (1) *binary* mixtures (four) of pure simple HCs to identify linear and nonlinear interactions with ethylene and other HC fuel candidates, and also (2) *ternary* mixtures (two) of simple HCs that included a vaporized liquid (*n*-heptane) at elevated temperature.

Thus, subsequent to some early experimental, analytic and numerical studies of opposed jet flows and HC/H_2 combustion [50-54], there has been increasing interest in HCs, both pure and mixed [3-25,42-49,55-58], and especially ethylene -- due to its high FS reactivity [45], and its continuing potential as a scramjet fuel component [13,16-19,59-62]. It has therefore been important to extend the exploration of ethylene and other HC FSs. Reference [63] examined the FS of additional mixtures of both gaseous and vaporized pure HCs (discussed below), and the writer's most recent study [64] investigated *for the first time* the Dynamic Flame Weakening (DFW) of two surrogate mixtures and their ethylene and methane components (including the recommended "64/36" surrogate), at various frequencies from 10 to 1600 Hz.

OJB Characterizations of HCs that Defined the "64/36" Surrogate

Ref. [63] first characterized the top-down methodology used to define simple gaseous surrogate hydrocarbon (HC) fuel mixtures for hypersonic scramjet combustion subtask 2 of the HIFiRE program. Ref. [63] then presented new and updated OJB extinction-limit FS data obtained from laminar non-premixed HC vs. air counterflow diffusion flames at 1-atm, which followed from earlier investigations. The FS results helped to characterize and define three candidate surrogate HC fuel mixtures that exhibited a common FS 70 % greater than for vaporized JP-7 fuel. These included our binary surrogate fuel mixture of 64 % ethylene + 36 % methane, which was our primary recommendation. It was (and is) intended to mimic the "critical flameholding limit" of a thermally- or catalytically-cracked JP-7 "like" fuel in HiFIRE scramjet combustion tests.

Our supporting experimental results in [63] included several key results and findings: (1) An idealized kinetically-limited ASR reactivity scale, which represented "maximum strength" non-premixed flames for several gaseous and vaporized liquid HCs; (2) FS characterizations of Colket and Spadaccini's suggested ternary surrogate, of 60 % ethylene + 30 % methane + 10 % *n*-heptane, which matched the ignition delay of a "typical" cracked JP fuel; (3) Data showing how our recommended "64/36" surrogate had an identical FS; (4) Data that characterized an alternate surrogate of 44 % ethylene + 56 % ethane with identical FS and nearly equal molecular weights. Although this could be useful when systematically varying the fuel composition, the mixture liquefies at much lower pressure, which limits on-board storage of *gaseous* fuel; (5) Dynamic Flame Weakening results that showed how oscillations in OJB input flow (and composition) can weaken (extinguish) HC vs. air flames up to 200 Hz, but the dynamic weakening for the "64/36" surrogate

was ~ 2.5 times smaller compared to pure methane; and finally, (6) FS limits at 1-atm that compared with three published 1-D numerical OJB extinction results using four chemical kinetic models. The methane kinetics generally agreed closely at 1-atm, whereas, the various ethylene models predicted extinction limits that averaged ~ 45 % high, which represented a significant problem for numerical simulation of surrogate-based flameholding in a scramjet cavity. Finally, we continued advocating the FS approach as more direct and fundamental for assessing idealized scramjet flameholding potentials than measurements of "unstrained" premixed laminar burning velocity or blowout in a Perfectly Stirred Reactor.

Arc-Heated Scramjet Test Facility Effects on Ignition and Flameholding

In 2002 one of the authors (GLP) conducted a detailed review and analysis of more than 100 papers on the physics and chemistry of scramjet ignition and flameholding combustion processes, and the known effects of air vitiation on these processes [39]. The paper attempted to explain vitiation effects in terms of known chemical kinetics and flame propagation phenomena. Scaling methodology was also examined, and a highly simplified Damköehler scaling technique based on OH radical production/destruction was developed to extrapolate ground test results, affected by vitiation, to flight testing conditions. The long-term goal of this effort was to help provide effective means for extrapolating ground test data to flight, and thus to reduce the time and expense of both ground and flight-testing. The same paper was also published as a Chapter, entitled "Air Vitiation Effects on Scramjet Combustion Tests," as part of the final report of the NATO RTO AVT WG-10 Scramjet Subcommittee [40]. Limited excerpts from this work are included and discussed below, especially as related to the present use of the AHSTF and the production and possible roles of nitrogen oxides and other air contaminants

Nitric oxide, NO, produced in amounts of 0.3 to 3 mole-%, can exert particularly strong effects on ignition, and to a lesser extent, on flameholding processes for high speed combustion applications with relatively low input-air temperatures [39,65,66]. Nitric oxide results from any high-temperature combustion, and especially arc heating processes involving air. In the AHSTF, arc-heated air is rapidly mixed with clean dry air just before expansion through a facility nozzle, and is processed by the scramjet inlet, isolator, and combustor. The resultant NO_x (estimated most often in simulations, less from experiments) promotes autoignition, which varies as a function of *T*, *P*, and equivalence ratio [67-70]. Note the percentage of NO_x needed for significant reduction of ignition delay approaches 1 %, which is close to the upper 'thermal' NO_x limit for a well-designed HC-preheated wind tunnel. Note also, a theory of the effect of additives on HC combustion [71] defined families of NO_x-releasing molecular species that are typically very effective combustion promoters. Thus, given our lack of detailed NO_x-effects data on scramjet ignition and flameholding over a useful range of *T*, *P*, and input composition/flows -- and considering the typical diffusive flame character of H_2–air and (much more complex) HC–air flameholding – it was conjectured that NO_x in HC-vitiated air may have strong and unexpected effects on scramjet HC combustion [65], and that further work was needed.

Slack and Grillo investigated the sensitization of H_2-air ignition by NO and NO_2 using a reflected shock tube technique [67]. They found an order-of-magnitude reduction of the ignition-delay induction period with ~ 0.5 mole-% NO or NO_2 at < 1000 K and 2 to 1 atm. Sensitization occurred via the Ashmore and Tyler mechanism [72]: Initiated by $HO_2 + NO \rightarrow OH + NO_2$, $H + NO_2 \rightarrow OH + NO$, and also $H_2 + NO_2 \rightarrow HNO_2 + H$ when NO_2 is present; supported by $H_2 + OH \rightarrow H_2O + H$; and terminated by $OH + NO + M \rightarrow HNO_2 + M$ and $OH + NO_2 + M \rightarrow HNO_3 + M$. Sensitization was most pronounced in the vicinity of the second explosion limit for H_2-air, where rates of $H + O_2 + M \rightarrow HO_2 + M$, and $H + O_2 \rightarrow OH + O$ are balanced at the classic "crossover" temperature; e.g. ~ 925 K at 1 atm, and autoignition becomes possible.

Test facilities may also introduce metallic / condensed-oxide species in the airstream. For example, arc heating typically releases copper vapor and oxide particles [66]. Even the stainless steel walls of shock tubes may release nickel-containing particles via shock tube erosion [73]. Fortunately, copper and nickel appear to be ineffective recombination catalysts in H_2–air flames (and possibly in HC–air flames), based on a detailed study of metal oxide/hydroxide catalysts. A ranked

listing (most efficient elements down to neutral ones) includes Cr, U, Ba, Sn, Sr, Mn, Ca, Mg, Fe, Mo, Co, and then Cu and Ni which are effectively neutral [74]. Note, however that Cr, a significant component of stainless steel, was found most efficient, and probably acts heterogeneously [74].

A recent paper [75] reviewed some known effects of metals on ignition, as studied in shock tubes and flames. Based on ignition delay calculations, it was shown that gaseous iron compounds such as $Fe(CO)_5$, Fe, FeOH, and FeO can affect the ignition delay of stoichiometric and fuel lean H_2–air mixtures near 1000 K and 1 atm. For example 1 ppmv (parts per million by volume) of iron could reduce the ignition delay by ~ 33 %, with peak reductions of a factor of two or three near 50 ppmv. The paper concluded: "The form of iron has a large effect on the promotion action, with FeO the most effective moiety tested. The promotion occurs from reactions of the iron compounds with H_2 or O_2, which lead to radicals (H, O, or OH) at early times, which then accelerate the subsequent build-up of HO_2 in the system. In addition to lowering the ignition delay, the iron compounds also lowered the cut-off temperature above which rapid ignition occurred. Above ~ 100 ppmv of additive, the iron compounds inhibit ignition, and the mechanism is similar to the gas-phase catalytic radical recombination cycles found to be important in laminar flame inhibition by iron compounds" [75].

Inert particle effects on combustion were recently analyzed theoretically [76,77]. The heat sink effect was found negligible (dust must exceed 10 % of total mass flow to exert an impact), but the effect on radical termination (recombination) on particle surfaces became important at dust mass fractions > 0.001 and particle sizes < 3 microns. At sufficiently high temperatures these phenomena are reduced by substrate softening that prevents particles from being eroded.

Charged and electronically excited molecular species may also influence test results. In arc-heated wind tunnels oxygen and nitrogen ions can be present. In general, their concentrations should be relatively low because Coulomb forces are long-range, and recombinations of positive ions and electrons are very fast. However, some neutral electronically excited species survive for long times. An example is O_2 in the singlet delta state, a species observed during either homogeneous third-body or surface catalytic recombination of O. This state of O_2 can persist for the order of seconds [78]. At present, relatively little is known about the possible effects of electronically excited species on combustion kinetics. However, if present in critical concentrations, they may reduce ignition delay time, because typical recombination / relaxation energies tend to be very high (of order 10 eV vs. 1 eV for recombination of radicals). Finally, ions can be exploited locally to promote combustion and anchor a flame. Examples of past work in this area are by P. Tret'yakov at ITAM in Novosibirsk; and T. Wagner and W. O'Brian at Virginia Tech. in Blacksburg, VA.

Content of the Present Paper

This paper focuses first on characterizing the effects of Arc-Heated contaminated air on the Flame Strengths of the "64/36" ethylene / methane surrogate fuel, and also pure ethylene and methane fuel, as a means of assessing possible impacts on flameholding during scramjet engine tests being conducted as subtask 2 of the HIFiRE program. As part of this process, we characterize the effects of nitric oxide (to > 3 %), and the effects of modest reductions in O_2 concentration (e.g., from 21 to 18.5 mole-%) on the FSs of the 7 gaseous HCs studied.

Four major purposes are served by the new FS (ASR) results: (1) Data from the pure HCs and "64/36" mixture provide additional sensitive and accurate means of validating, globally, complete and reduced chemical kinetic mechanisms. These apply at the critical flame core temperatures that determine non-premixed flame extinction, and also at the moderately elevated fuel inflow temperatures that are typically required to maintain fuel vapor; (2) The experimental FS and ASR normalized results, while being directly helpful in validating and refining kinetic mechanisms, further support semi-quantitative assessments of the robustness and loss of "incipient" flameholding in scramjet combustors, for both the pure and mixed HC fuels over wide ranges of reactivity; (3) The originally defined binary gaseous surrogate fuel effectively allows substitutional bypassing of relatively complex vaporization and catalytic cracking system designs in test systems where supersonic combustion (scramjet) operability is the major goal; and perhaps most importantly, (4)

The possibility of using binary surrogate mixtures of *variable* composition continues to offer important additional flexibility and research value for scramjet tests; i.e., mixtures allow well-defined and easily attained means of varying fuel reactivity through changes in ethylene composition to effectively map the limits of robust and weak flameholding performance *with fixed geometry designs*.

The experimental section below describes the methodology used to characterize the FSs of all the HC vs. clean-air systems investigated, and also the respective effects of NO and reduction of O_2 concentration on the FSs of HC vs. NO- and N_2-contaminated airs for the 7 gaseous HCs studied.

EXPERIMENTAL

Schematics, with detailed descriptions, are given for the nozzle-OJB system that was originally used (vertical orientation with a selectable Oscillatory-inflow delivery) in the Oscillatory Opposed Jet System (OOJB) in Fig. 1a; a recent horizontal tube-OJB system, Fig. 1b; and an associated liquid HC vaporizer-accumulator-OJB system, Fig. 1c. All three systems depict the use of convergent Pyrex nozzles, and long nickel or stainless steel tubes (50 to 100 diameters in length), of the same size and type. No guard flows were used (or seemed to be needed) at the typical flow rates employed for extinction of thin disk-shaped flames. Although horizontal configurations sometimes showed a slight flame asymmetry due to buoyancy (but negligible differences in results) [33], they favored formation of resultant ring-shaped flames, and thus allowed measurements of flame restoration, which approximate a slightly strained laminar burning velocity (discussed below). Each ceramic fiberboard combustion box had Pyrex windows, and a porous sintered metal plate over the top. Nitrogen (or argon) entering through diffuser-jets at the bottom of each box reduced extraneous combustion outside the central impingement region, and thus minimized adverse buoyancy and visibility effects. Fuel and air component flows were hand-controlled with micrometer valves, and measured by mass flow meters calibrated for air at 0 ^{o}C, 1-atm pressure. Vendor-published mass flow meter correction factors (either measured relative to air or evaluated as ratios of heat capacities) were used for calculating mole fractions of HC mixtures involving ethane, propane, butane and propylene. Similar published factors for methane and ethylene were found in significant error, and were thus evaluated independently in a series of carefully controlled experiments [45].

To attain extinction (blowoff) of a stabilized gaseous fuel–air disk flame, the fuel flow rate was gradually increased (or, for N_2 diluted fuels, fixed at a target rate as N_2 diluent was increased); simultaneously, the airflow was gradually increased, so that the flame was always centered and free-floating (fully responsive to small differential changes in flow rates). Upon sudden blowoff, a ring-shaped (torus) flame sometimes stabilized. After mass flows of each component were recorded, gradual flow reductions led to slow closure of the ring flame, and eventually, to sudden disk restoration (see Ref. 26 for a summary of the author's earlier CFDF restore results, and Ref. 58 for a recent independent study). Extinction data were almost always obtained in duplicate, and were sometimes replicated 10 or more times, especially in the case of heated / vaporized liquid fuels. Here, premixed (with N_2, or one or two gaseous HCs) vaporized-HC flows from the pressurized accumulator system, Fig. 5c, were simply varied in tandem with flows of air to achieve extinction. Similar procedures were applied for mixed gaseous H_2/HC–air and HC_1/HC_2–air systems, in that H_2 or one HC diluent / reactant was fixed, while the other was gradually increased in tandem with air to achieve extinction.

The flow system and procedures used for introducing NO and N_2 (hereafter denoted N_2*) contaminants were identical throughout the study, from the point where a dedicated hand-controlled micrometer valve (not shown) was used to deliver a pre-determined mass flow rate of contaminant. In each experiment, a steady contaminant flow was blended downstream with a slowly increasing flow of air, until flame extinction occurred. The system just downstream of the micrometer valve consisted of a dedicated mass flow meter (calibrated for air at 0 ^{o}C, 1-atm); 90 cm of 6 mm i.d. stainless steel tube that led to a 90-degree mixing tee (6 mm i.d.), where opposed flows of clean air and contaminant mixed; ~ 50 cm of 6 mm i.d. flexible (ribbed) stainless steel tube; 52 cm of 9 mm i.d. thick-wall neoprene tube; and finally 48 cm of 9.3 mm i.d. horizontal aluminum tube that

terminated in the combustion box to deliver a steady laminar jet of contaminated air with a tube separation of 12-14 mm. Note the mixing of NO with air must be done "on the fly" to suppress conversion of NO to NO_2 to a practical minimum, via the (unusual) ternary reaction, NO + NO + O_2 → 2 NO_2, which varies (in rate) as the square of NO concentration.

Reported exit cross-section-average jet velocities, U_{air} and U_{fuel}, are calculated from the measured component mass flow rates, flow meter calibration factors for each gas, and carefully measured nozzle or tube exit diameters. Mass flow meter calibrations of airflow rates are referenced to 0 ^{O}C and 1-atm, but are then corrected to 300 K (ideal gas law) and 1-atm [44]. Corresponding Reynolds numbers for air (Re_{air}) based on diameter were generally less than 1500, but considerably lower values were avoided; especially because flames can become excessively thick when vertical, and also non-axisymmetric when horizontal, due to buoyancy. Radiation effects were considered negligible at the relatively high strain rates used.

The matched tube-OJBs (9.3 and 7.56 mm diameter recently, but ranging from 2.7 to 10.0 mm in previous studies) were mounted horizontally. The 7.2 mm Pyrex nozzles were mounted vertically, with both elements insulated to reduce heating of the inflowing gases.

The 9.3 mm (and 7.5 mm) tube- and 7.2 mm nozzle-OJBs were spaced 1.7 to 2 exit-diameters apart (note that the extinction limits are exceptionally independent of jet separation distance beyond one diameter, and sometimes up to 4 diameters [26]). For measurements with H_2, both 2.7 and 2.91 mm OJB's were spaced 7 mm apart to ensure free-floating finite-thickness flames, free of significant flame attachment / anchoring effects. Flow rates were generally high enough that buoyancy and OJB orientation effects on flame extinction appeared negligible [26,33,43-45] whenever data were recorded. When used, vaporized-HC fuel mixtures flowed through the electrically heated vaporizer and accumulator tanks and tubes with thermocouple monitoring (see Fig. 1c), before entering the OJB combustion chamber, so that these fuels were heated up to ~ 600 K to prevent condensation.

Errors in extinction limits stemmed from various sources. In earlier air-contaminant studies of the H_2–air system, *absolute* strain rates at extinction (not density weighted) were predicted (1-D) to vary linearly with input temperature, up to ~ 600 K [52,54], and *absolute* ASRs for heated H_2–air, using a 2.7 mm tube-OJB, were found to vary "nearly" linearly (e.g., with only a 14% excess increase in density-weighted ASR from 300 to 600 K [38]). Thus, direct measurements of mass flow rates effectively negated most effects of variable jet temperature on *absolute* jet velocity via the ideal gas law. This led to significant reduction of data scatter, especially when input heating was required. Atmospheric pressure variations caused small variations of U_{air} extinction limits that were generally ignored and averaged-out during earlier hydrogen studies [26], but more recent HC and H_2 data were corrected by applying a dimensionless pressure factor of $(1/P)^{+3}$ [44]. Calculated (density-weighted) jet exit velocities at standard conditions varied inversely as the square of measured D, and ASRs varied as D^{-3}. Finally, un-reconciled small differences between the data sets were due to earlier unmeasured variations in atmospheric pressure, differences in centering flames, daily jet realignment, sporadic but generally small mass flow meter drift, periodic mass flow meter calibrations, small transient cooling / heating flow response effects in flow meters, and differences in the spatial distribution and flow rates of argon or nitrogen purge flows in the combustion box.

In summary, relatively ideal and well characterized 9.3 (and 7.56 mm) tube-OJB and 7.2 mm nozzle-OJB systems were the primary tools used and cited in this study for assessing strain-induced extinction limits of gaseous HC–air CFDFs using both clean and systematically-contaminated air.

RESULTS AND DISCUSSION

Extinction Limits for HCs with N_2* Dilution of Air (Oxygen Depletion Effect)

Fig. 2 shows the Applied Stress Rate (ASR) extinction data obtained from systematic N_2* dilution (N_2 contamination) of air, for six pure HC fuels and two "64/36" surrogate fuel mixtures, using a 9.3 mm Tube-OJB with 1-atm, 300 K inputs. Flame extinction occurred at each data point, and thus respective data define upper applied-strain-rate flame boundaries, beyond which quasi-steady (or oscillatory) laminar flames cannot exist. The linear data fits are considered excellent and appear entirely adequate (no parabolic fits required). Because the systematic dilution of air with N_2* causes the O_2 content to decrease proportionally [mole-% O_2 = 20.95*(100 – mole-% N_2*)/100], it is clear from the data that the reduction of O_2 content has a *strong* effect on the extinction limit of every fuel tested. As a footnote, butane has been observed to deviate noticeably from the other hydrocarbons in the author's studies of "steady" flame extinction [63], dynamic flame weakening [64], and also in reported studies of blowout in a Perfectly Stirred Reactor and burning velocity [82]. Later on, the slopes are normalized by respective intercepts to assess percentage changes in ASR with N_2* dilution that correlate directly with decreases in O_2 concentration.

Previously, individual ASR data for the two surrogate mixtures (commercial premixed bottles received 7/2/09 and 9/17/09) were analyzed separately for both N_2* and NO dilution of air using the 9.3 mm OJB. The respective zero-contamination ASR intercepts were 133.50 and 138.09 1/s for N_2* dilutions, and 134.47 and 133.60 1/s for NO dilutions. The N_2* dilution results were also compar-ed with recent 7.56 mm OJB data on the 7/2/09 bottle, and with our previously published ASR data on ethylene, methane, and "64/36" surrogate mixtures prepared by using the lab mass flow metering system and the 7.56 mm OJB [63]. After the respective ASR intercepts and independent ASRs were compared on a proportional basis, and with certified analyses of the surrogate bottles, it was found that the "reduced OJB data" and certified analyses generally agree within $\pm$ 2 % and in some cases within 1 %. Thus, based on the detailed measured variations in ASR with ethylene mole fraction [45,63], the presently deduced variability in results between bottles and with the target extinction limit is well within expected limits, and is considered entirely acceptable for testing.

Fig. 3 shows the same ASR extinction data as in Fig. 2, except the respective results are expressed in terms of changes in O_2 concentration from our standard dry-clean-air value of 20.95 % O_2. These results explicitly illustrate some remarkably high sensitivities of extinction ASRs to O_2 concentration; e.g., for the "64/36" surrogate, normalization of the slope by the intercept leads to a 19.0 % decrease in ASR per unit decrease in mole-% O_2. This remarkably high oxygen sensitivity for extinction of the "64/36" surrogate is *2.5 times larger* than observed much earlier for hydrogen fuel [34,38], as described below.

In the case of H_2, an extensive set of 100 % H_2 vs. contaminated-air extinction results from a 2.7 mm Tube-OJB, with variations in mole-% O_2 over the range 16.5 to 30 % O_2, led to a 7.49 % decrease in ASR per unit decrease in mole-% O_2 [34]. Furthermore, the 7.49 sensitivity (for non-premixed CFDF extinction limits) was virtually identical to the sensitivity of burning velocity (7.35), as derived by this writer (GLP) from published burning velocity data for hydrogen [56]. Finally, later in the paper, it will be shown that the sensitivities of ASR extinction limits to oxygen for HCs in Fig. 3 are similarly comparable to those for published HC maximum flame velocities.

Fig. 4a shows resultant sensitivities of ASR extinction limits for all seven HC fuels to increases in percent N_2* content, and Fig. 4b shows sensitivities for the same data to decreases in percent O_2 content. The respective sets were derived by normalizing the slopes in Fig. 2 and 3 with corres-ponding intercepts, and expressing the results as percentage changes in ASR per unit mole % N_2* in the contaminated air mixture, or mole % decrease in O_2 in the mixture. Both plots show the high sensitivities for methane dominate the response of the "64/36" surrogate, compared to somewhat lower sensitivities for ethylene. Sensitivities for the five other HCs generally fall between those for methane and ethylene, with butane having a somewhat reduced sensitivity, as discussed earlier.

In view of the newly found high sensitivities to oxygen depletion for ASR (and FS), for all the HCs tested, some practical suggestions for high speed airbreathing propulsion applications are immediately apparent. First, it is clearly important to maintain tight control of oxygen make-up in vitiation facilities that restore oxygen content. Second, local variations in content between the core of high-speed flows and mass averaged flows could cause significant differences in localized flameholding limits. Third, since the new results show that oxygen sensitivities for hydrocarbon fuels are ~ 2.5 times larger than they are for hydrogen, it is especially important to re-examine the possible roles of oxygen deficiency on localized HC–air flameholding in new testing of high speed combustion applications.

An alternate graphical illustration of the sensitivities for O_2 depletion in Figs. 4a and 4b is shown in Fig. 5. In this case the results are converted to fractional "O_2 depletion" effects for the consumption of oxygen from 20.95 % O_2 to 19.45 % O_2 when 3 mole-% NO is produced in the Arc Jet processed air. Thus for any given O_2 mole fraction, $X(O_2)$, the fractional "O_2 depletion" effect is simply defined as the ratio, $[ASR(X(O_2))] / [ASR(0.2095)]$. The results for ethylene, methane, and the "64/36" surrogate mixtures are used later to deduce projected net effects on flameholding for Arc-Heated-heated air.

Finally, in light of the significant fractional sensitivities for "O_2 depletion" shown above, we especially note the factors of 0.71 found for methane and the "64/36" surrogate, which increase to 0.78 for pure ethylene. Later, it will be evident that these large "O_2 depletion" effects tend to dominate over much smaller and less variable "NO enhancement" effects, deduced below.

Extinction Limits for HCs with NO Dilution of Air (NO Enhancement Effect)

Fig. 6 shows the ASR extinction data obtained from systematic nitric oxide (NO) dilutions (contamination) of air, for ethylene, methane, and the two "64/36" surrogate fuel mixtures, using the 9.3 mm Tube-OJB system in an identical manner compared to the N_2* dilution work in Figs. 2 and 3. As before, data were combined for the two surrogates. Good linear fits of the methane and the combined "64/36" mixture data were obtained, but the ethylene data clearly required a parabolic fit. The individual fits of the "64/36" mixture data (not shown) were nearly identical (notably, data were obtained the same day). Note the maximum (endpoint) NO concentrations for the respective fuels vary systematically from (just over) 4 to 6 to 8 %. This progression reflects use of the same maximum diluent flow in each experiment.

Next, the fractional "NO enhancement" effect was deduced for each of the three fuels shown in Fig. 6, as follows. For any given mole fraction of NO in air, X(NO), compared to an *identical* mole fraction of added nitrogen, $X(N_2*)$, the "NO enhancement" effect could be deduced by the ratio $[ASR(X(NO))] / [ASR(X(N_2*))]$, since the extinction data for NO and N_2* additions to air were conducted under identical conditions. The resultant fractional "NO enhancement" effect on ASR at extinction, for 3 mole % NO (maximum value expected) and ethylene, methane and the two "64/36" surrogate fuels is 1.029, 1.017, and 1.043, respectively, based on the data in Fig. 6 for NO and Fig. 2 for N_2*.

Although more detailed results for lower NO concentrations are shown in the next section, it is already apparent that the "NO enhancement" effect is very small compared to a growing "O_2 depletion" effect that results at higher Mach numbers, as NO concentrations approach 3 mole-% and higher. This surprisingly small NO effect can be compared to earlier numerically-deduced effects on HC combustion that were projected as possibly being more than an order of magnitude larger, as conjectured in an earlier review [65].

Analysis of O_2 Depletion and NO Enhancement Effects for Arc-Heated Air

The net effect on ASR at extinction, for ethylene, methane, and the "64/36" surrogate fuels vs. Arc-Heated-contaminated air can be deduced from the above OJB-derived "NO enhancement" and "O_2 depletion" effects to Arc-Heated air, as follows. First, we assume that Arc-Heated air has a

simplified composition, in which each mole of NO produced in the arc is derived from the consumption of 1/2 mole each of O_2 and N_2, and no other important chemistry occurs. In this case a material balance shows that the net number of moles of air is unchanged.

Second, we make a primary assumption that the "net" fractional effect on ASR is simply the product of the "NO enhancement" and "O_2 depletion" fractional effects, and there are no significant secondary interaction effects, e.g., in which the presence of NO alters the "O_2 depletion" effect. This assumption could have been tested *if* extinction measurements had been obtained by *simultaneous* variation in NO and O_2 concentrations to correspond to the assumed simplified air composition. Nevertheless, the absence of significant secondary effects seems quite reasonable for the OJB air dilution experiments, considering (1) the OJB-measured "NO enhancement" effect is comparatively small up to 3 % NO, and (2) the basic Ashmore and Tyler mechanism for NO "catalysis" of flames, based on hydrogen and oxygen radicals, should be relatively insensitive to a small reduction in O_2 concentration when 3 % NO is added (e.g., from 0 to 0.97*20.95 = 20.32 % O_2).

Despite the above simplified assumption, the problem of mimicking *actual* perturbations of Arc-Heated-processed air may be much more difficult. First, on the one hand, because the O_2 and N_2 reactants are in relatively large excess within the electrical arc, and the concentration of NO produced is strongly related to peak temperatures, the actual NO produced should not be perturbed significantly by the relatively small reductions of O_2 and N_2 reactants. Second, however, co-produced metastable oxygen, with a significant lifetime in the electronically excited delta O_2 state as noted earlier [78], may survive the subsequent rapid mixing with clean dry air, followed by supersonic expansion through the facility nozzle that would help freeze the metastable composition. If delta-O_2 does survive the mixing and expansion, it would surely enhance ignition kinetics, and possibly affect flameholding reactivity.

Finally, the effects of copper vapor represent an additional unknown, although our original review [65] suggested that copper vapor is relatively benign in hydrogen and oxygen containing flames, compared to some elements, such as chromium. Presently we cannot account for possible "excited state" effects without the benefit of a more complete literature survey, detailed considerations of possible reactions of charged and/or metastable neutral species with hydrocarbons, and some key experimental data.

If we now bypass the above considerations, and accept our original assumption that the "net" effect on ASR at extinction is simply deduced as the product of OJB-derived "NO enhancement" and "O_2 depletion" effects to Arc-Heated-like air, it is important to use the *actual* projected O_2 concentration that should occur. Thus, for our limiting case of 3 % NO in Mach 7 Arc-Heated air, the O_2 concentration should decrease from 20.95 % to 19.45 % O_2. However, in order to realize this O_2 concentration in OJB "O_2 depletion" experiments, ASR data corresponding to N_2* = 7.160 % O_2 must be used to compute the corresponding "O_2 depletion" effect (instead of using 3 % added N_2* that only corresponds to 0.97*20.95 = 20.32 % O_2).

Thus for 3 % NO in Arc-Heated air, the projected "Net" fractional effect is determined from OJB ASR extinction data as follows:

("net" effect) = ("NO enhancement") ("O_2 depletion")

("net" effect) = [ASR(3 % NO)] / [ASR(3 % N_2*)] [ASR(7.16 % N_2*)] / [ASR(0 % N_2*)]

Fig. 7 shows the resultant "fractional effects" on ASR at extinction obtained for 3 % NO in Arc-Heated air as a function of ethylene content in the fuel. Note because there are only three fuel compositions, line segments are used in lieu of curve fits. Methane shows a large "O_2 depletion" effect (0.71) that appears to dominate the behavior of the "64/36" surrogate (0.71) before the effect on ASR becomes slightly reduced for ethylene (0.78). Because the "NO enhancement" effect is relatively small for the three respective compositions (1.02, 1.04, 1.03), the "net" effect is only slightly larger (0.72, 0.74, 0.81), and is clearly dominated by the "O_2 depletion" effect.

Finally, Fig. 8 is a comprehensive plot of deduced "fractional effects" results for the "64/36" surrogate and pure ethylene, as a function of mole-% NO in Arc-Heated-like air, up to 4 % NO. Based on previous survey measurements [66], a free stream Mach number of 7 is projected to produce 3% NO. While the "O_2 depletion" effects are strictly linear with NO concentration, both the "NO enhancement" and "net" effects are very nearly linear. Whereas the "NO enhancement effect is generally small, and increases only slowly with NO concentration, the "O_2 depletion" effect is roughly seven times larger for the "64/36" surrogate at 3 % NO, and thus dominates the "net" effect.

Translation of global strain rates to absolute (local) axial input strain rates

In a previous paper [63] "easiest-to-measure" global OJB strain rates (ASRs), obtained from a 7.56 mm Tube-OJB, were translated into *more generalized* absolute (local) maximum axial input strain rates that occur near the airside edge of a CFDF. The local strain rates also represent the outputs of detailed 1-D and 2-D numerical simulations, subject to idealized boundary conditions. A similar (but much more difficult, and less certain) approach was taken for the translation of global OJB strain rates to radial strain rates *in the so-called flame core* (generally not located at the stagnation point). Flame-core radial strain rates should constitute the "truest representation" of the strength of CFDFs, but they are by far the most difficult to measure using non-intrusive laser diagnostics, and to model using more intensive 2-D simulations.

In Appendix A, details of the "original" translation [63] are first reviewed, due to the importance and difficulty of validating chemical kinetic models for the extinction of ethylene and "64/36" surrogate fuels at 1 atm. Then in the section below we characterize, translate, and incorporate the new extinction data that were obtained for the same seven fuels, using the slightly larger and more ideal 9.3 mm Tube-OJB. And finally the translated 9.3 mm data are superimposed on the original 7.56 mm data, and the original Fig. 9 plot is updated to reflect new numerical simulations, based on a newly revised / expanded chemical kinetic model (USC, 2009), and new independent extinction measurements for ethylene vs. air (at UVa). The measurements are based on ASR global inflow strain rates *and* the use of detailed Digital Particle Imaging Velocimmetry (PIV) to determine maximum local axial strain rates.

Development of the New Updated Translation of Extinction Limits

This new and updated translation first reviews how the new 9.3 mm Tube-OJB extinction results for the pure HCs compare with all the earlier ASR data obtained over several years for a wide range of tube diameters. Then the 9.3 mm results are overlaid on the 7.5 mm Tube-OJB results in Fig. 9 (discussed in Appendix A), after exchanging the original abscissa and ordinate scales to make a more realistic comparison.

First, Fig. 10 shows that the new 9.3 mm Tube-OJB extinction data compare favorably with (1) limited 1993 data [44] using the same 9.3 mm tubes, and (2) the ASR vs. tube diameter trends of previous extensive data obtained using several different size OJBs in different OJB systems over the last 20 years. The downward asymptotic approach of ASR for each fuel to approximate baseline values is important when comparing data with both 1-D Navier Stokes stream function solutions for infinitely large diameter uniform-flow nozzles, and with 2-D numerical solutions for finite diameter convergent nozzles (plug inflows) and straight tubes (parabolic inflows).

Next, Fig. 11 shows the re-plotted updated version of Fig. 9 (with axes reversed) that now contains all the new 9.3 mm Tube-OJB data co-plotted against the earlier 7.2 mm Nozzle-OJB data, and overlaying the earlier 7.5 mm Tube-OJB data first presented in [63]. Note that a slightly larger K_t factor of 5.9 was required to shift and co-plot the 9.3 mm Tube data with the (smaller diameter) 7.2 mm Nozzle data, compared to the K_t factor of 5.1 used for the earlier 7.5 mm Tube data. This increase in K_t factor from 5.1 to 5.9 seems quite consistent with the downward trend in ASR results with increasing tube diameter, shown in Fig. 9.

Fig. 11 also contains two new result comparisons. First, a new independent experimental data point is shown from data obtained by Chelliah [79,80] on a newly developed 7.95 mm nozzle-OJB system, which included a Digital Particle Imaging Velocimetry (DPIV) system to survey nozzle flow profiles and obtain the airside maximum axial input strain rate at extinction. This result agrees within 5% of our original datum for ethylene presented in [63]. Second, a new numerical extinction strain rate is also shown to fall within 5% of the original datum for ethylene. The numerical result was obtained by Chelliah [79,80] after using a new 2009 USC chemical kinetic model developed by H. Wang et al. [81]. The 2009 model was expanded from an earlier 2007 USC model [81] that had 71 species and 469 two-way reactions, to a more comprehensive model having 111 species and 784 two-way reactions. The Egolfopoulos experimental result, which differs from the present experimental and numerical results, was obtained independently at USC in 2008 (see [79]) using PIV to determine the maximum axial strain rate at extinction.

Based on the updated results in Fig. 11 it can be seen that (1) our nearly-coincident 2008 and present extinction data for ethylene, and the new UVa experimental data agree remarkably well (within $\pm$ 5 %), and (2) the experimental data exhibit a similarly good level of agreement with the new numerical result [79,80] obtained using the new 2009 USC chemical kinetic model [81]. Furthermore, there was similarly close agreement with methane (with good agreement dating back more than a decade [26]). Finally, due to the duality of extinction data in Fig. 11 based on plug and parabolic inflows, and incorporating four other pure HCs and the "64/36" surrogate, we conclude that the various experimental results in Fig. 11 offer excellent bases for the global validation of other chemical kinetic and molecular diffusion models on the entire set of hydrocarbons studied.

Relative Effects of O_2 Depletion on ASR Extinction *and* Burning Velocity

Finally, it is informative to compare the present strong relative effects of O_2 depletion on extinction of non-premixed HC vs. air flames, with the relative effects of O_2 on the maximum burning velocity of simple HC fuels premixed with synthetic O_2 / N_2 mixtures. Some early extensive burning velocity measurements for ethylene, methane and propane in [82] illustrate the substantial effects of O_2 concentration, on 'both sides' of 21 % O_2, on "maximum flame velocity" at room initial temperature and 1-atm. These were measured using the "schlieren total area method" (and also other methods), as documented in Figure 140 and Table XIII of Ref. [82]. Note these data do not incorporate the detailed corrections for effects of strain on burning velocity that have been developed in recent years, but this should not significantly affect the comparisons described below.

Fig. 12 shows the present relative effects of oxygen dilution on ASR at extinction for ethylene, the "64/36" surrogate, and methane (in terms of mole-% N_2* diluent) compared with the relative "maximum flame velocity" results. Note the flame velocity data for ethylene and methane vary linearly with N_2* dilution.

The most important features of the Fig. 12 comparisons are: (1) relative maximum flame velocity has nearly as strong a dependence on O_2 concentration as ASR does, which is explicitly noted in [82] to be much larger than observed for hydrogen, and (2) the respective relative results for methane and ethylene ASR and flame velocity follow similar trends with O_2 dilution/reduction, and differ by roughly the same proportion; i.e. ethylene is affected somewhat less by O_2 depletion than methane, to roughly the same degree with both sets of results.

In conclusion, (1) the present ASR extinction results for ethylene, methane, and other simple gaseous HCs show large and very significant sensitivities to oxygen depletion, compared to hydrogen (~ 2.5 times smaller), and (2) maximum burning velocities of similar premixed fuel/air systems show comparably large sensitivities to oxygen depletion, that are also much larger than for hydrogen combustion.

Therefore, on a practical note, one important facet of the above findings for testing scramjet combustors, is to recognize that ongoing and future tests with hydrocarbons may depart significantly

from previous experiences with hydrogen fueled scramjets (e. g. Hyper X) in high-temperature facilities that deplete oxygen and/or use oxygen make-up.

CONCLUDING REMARKS

The present work is a major extension of a May 2008 JANNAF paper (and earlier ones) that characterized several pure HC and surrogate (mixture) fuels for the HIFiRE project, that were designed to mimic the flameholding of reformed (thermally- or catalytically-cracked) endothermic JP-like fuels. The normalized Flame Strength approach used represents a continuation of earlier work on hydrogen, air contaminants, and three surrogate HC fuels. The methodology is applied as a fundamental and practical "best measurement" for assessing idealized scramjet flameholding potentials for clean and high enthalpy contaminated air. This is because normalized-FS (ASR) *directly* measures a chemical-kinetic-dominated, diffusion influenced, strain-rate-sensitive limit of non-premixed combustion at typical incipient-flameholding temperatures. Thus, it approximately mimics conditions where gaseous fuels are injected (and transported from upstream injection) into a subsonic flameholding recirculation zone, and mixed with compressed and shock-processed air captured from an upstream inlet. Although only a fraction of the overriding flow is captured and reacts with the locally injected fuel, the effects of local aerodynamic strain and associated multi-component diffusion on incipient flameholding-combustion remain key to maintaining scramjet combustion.

Some new and unique nitric oxide (NO) and oxygen air-contamination effects on the extinction Flame Strength (FS) of non-premixed hydrocarbon (HC) vs. "air" flames are characterized in this paper for 7 gaseous HCs, using a new idealized 9.3 mm straight-tube Opposed Jet Burner (OJB) at 1 atm. Besides ethane, propane, butane, and propylene, the HCs include ethylene, methane, and a 64 mole % ethylene / 36 % methane mixture, our previously recommended gaseous surrogate for fueled HIFiRE scramjet tests. The new FS data for the undiluted gaseous HCs are consolidated with previously validated data (May 2008) normalized to absolute (local) axial-input strain rates, and are co-plotted on a dual idealized, kinetically dominated reactivity scale. Excellent agreement with prior data is obtained for all 7 fuels. Detailed comparisons are made additionally with recently published (UVa) numerical results for ethylene extinction. A 2009-revised (USC) ethylene kinetic model led to numerically predicted limits within ~ 5 % (compared to 45 %, earlier) of this writer's 2008 (and present) ethylene FSs, and also with recent comprehensive data obtained on a new independent OJB system (UVa). These agreements, and a hoped-for "near-identically-performing" reduced kinetics model of sufficiently small size should greatly enhance the capability for accurate numerical simulations of surrogate HC flameholding in scramjets.

The presently measured air-contamination effects on FS extinction limits are projected to assess AHSTF "facility test effects" of NO production (e.g., 3 mole-%) and resultant oxygen depletion (e.g., from 21 % to 19.5 %), for testing a "64/36" surrogate fuel in HIFiRE engine designs. The FS results show a generally small ($\leq$ 4 %) nitric oxide enhancement effect, relative to clean air, for up to 3 % NO (free-stream Mach number up to 7 in the AHSTF). However, a progressively large oxygen-deficiency weakening effect develops. For 3 % NO, a net weakening of 26 % in FS is derived for the "64/36" fuel vs. air, based on tube-diameter-normalized FSs (ASRs) and absolute (local) axial input strain rates. The corresponding net weakening for pure ethylene is 20 %.

The following conclusions are drawn from this study:

1. Very significant "oxygen-deficiency weakening" effects on ASR at extinction were accurately quantified for all seven HCs tested.

2. So-called "nitric oxide enhancement" effects on flame extinction limits are quite small (up to ~ 4 %) for both methane, ethylene, the "64/36" surrogate fuel mixture, and probably by extension, most simple gaseous HCs. The same was previously found true for hydrogen fuel.

3. Because the “oxygen-deficiency weakening” effects grow large, and are about 2.5 times greater that previously determined for hydrogen fuel, renewed attention needs to be paid to facility test effects that may alter local oxygen concentration in the central test core flow, such as in vitiated test facilities with oxygen make-up, and in Arc-Heated facilities that alter oxygen concentration by consuming it to produce NO.

4. The deduced 26 % reduction in normalized flame strength projected for the “64/36” surrogate fuel, vs. Arc-Heated-contaminated air containing 3 % NO, strongly suggests that in-flight flameholding limits may be strengthened by the same amount in a HIFiRE scramjet when flying in clean air. This may or may not become important, as long as the additionally-gained “robustness” of flameholding does not lead to a critical excess of upstream heat release, with a consequent significant shift in ramjet-to-scramjet mode transition, and/or the onset of an “unstart” condition.

5. The newly obtained ASR extinction limits for six pure gaseous HCs and the “64/36” surrogate fuel mixture agree exceptionally well with the author’s previously published results, determined for respective plug and parabolic inflows using somewhat smaller OJBs. The prior translation (2008) of these results to absolute (local) axial strain rates at extinction led to the conclusion that numerically deduced extinction limits, using a 2007 chemical kinetics model for ethylene, were about 45 % high. Since 2008, that conclusion appears to have been further validated by (1) the present experimental results, which agree closely with the earlier results for the same HCs, (2) a new, independent, Digital-PIV-supported extinction limit measured (at UVa) for ethylene, which agrees with our earlier data within 5 %, and (3) new numerical simulations (UVa), using an expanded and revised 2009 chemical kinetic scheme developed at USC, that now agrees within 5% of our experimental results.

Thus it is concluded that the present level of agreement ($\pm$ 5 %) is satisfactory, and a suitably reduced chemical kinetics set that produces essentially the same extinction results for ethylene at 1-atm as the new (2009) complete kinetics model, would permit detailed numerical simulations of flameholding in HIFiRE-like scramjet combustor designs.

6. It is possible that electronically excited long-lived metastable delta-O_2, which is very likely formed in the Arc-Heating, may survive the subsequent mixing with air and expansion through the facility nozzle, and may then persist through the inlet and isolator into the combustor. This possibility should be assessed for the AHSTF tests. Simple measurements may be possible. If present in significant concentrations, the delta-O_2 would surely affect autoignition the most; flameholding at higher temperatures would likely be less affected due to the presence of flame radicals and inherently higher enthalpy.

REFERENCES

1. Spadaccini, L.J., “Autoignition “Characteristics of Hydrocarbon Fuels at Elevated Temperatures and Pressures,” ASME Paper No. 76-GT-3, March, 1976, 5 pp.

2. Spadaccini, L.J., and TeVelde, J.A., “Autoignition Characteristics of Aircraft-Type Fuels,” *Combust. Flame* **46**, (1982), pp. 283-300.

3. Edwards, T., “USAF Supercritical Hydrocarbon Fuels Interests,” AIAA Paper 93-0807, Jan., 1993, 11 pp.

4. Maurice, L.Q., Corporan, E., Minus, D., Mantz, R., Edwards, T., Wohlwend, K. Harrison, W.E., Striebich, R.C., Sidhu, S. Graham, J., Hitch, B., Wickham, D, and Karpuk, M., “Smart Fuels: “Controlled Chemically Reacting Fuels,” AIAA Paper AIAA 99-4916, July, 1999, 11 pp.

5. Wickham, D.T., Alptekin, G.O., Engel, J.R., and Karpuk, M.E., “Additives to Reduce Coking in Endothermic Heat Exchangers,” AIAA Paper AIAA 99-2215, July, 1999, 9 pp.

6. Colket, M.B., III, and Spadaccini, L.J., "Scramjet Fuels Autoignition Study," J. Propulsion and Power, **17**, No. 2, 2001, Mar.-Apr. 2001, pp. 315-323.

7. Gruber, M. Dunbar, J., and Jackson, K., "Newly Developed Direct-Connect High- Enthalpy Supersonic Combustion Research Facility," J. Propulsion and Power, **17**, No. 6, Nov.-Dec. 2001, pp. 1296-1304.

8. Mathur, T., Gruber, M., Jackson, K., Donbar, J., Donaldson, W., Jackson, T., and Billig. F., "Supersonic Combustion Experiments with a Cavity-Based Fuel Injector," J. Propulsion and Power, **17**, No. 6, Nov.-Dec. 2001, pp. 1305-1312.

9. Quick, A., King, P.I., Gruber, M.R., Carter, C.D., and Hsu, K-Y., "Upstream Mixing Cavity Coupled with a Downstream Flameholding Cavity Behavior in Supersonic Flow," AIAA Paper AIAA-2005-3709, July, 2005, 13 pp.

10. Rasmussen, C.C., Driscoll, J.F., Hsu, Kuang-Yu, Donbar, J.M., Gruber, M.R., and Carer, C.D., "Stability Limits of Cavity-Stabilized flames in Supersonic Flow," Proceedings of the Combustion Institute **30** (2005), pp. 2825-2833.

11. Cooke, J.A., Bellucci, M., Smooke, M.d., Gomez, A., Violi, A., Faravelli, T. and Ranzi, E., "Computational and Experimental Study of JP-8, a Surrogate, and its Components in Counterflow Diffusion Flames," Proceedings of the Combustion Institute **30** (2005), pp. 439-446.

12. Maurice, L.Q, Edwards, T., Cuoco, F. Bruno, C, and Hendrick, P., CHAPTER 2: Fuels, in *Technologies for Propelled Hypersonic Flight*, RTO-TR-AVT-007, Volume 2 – Subgroup 2: Scram Propulsion, ISBNs 978-92-837-0041-4 / 978-92-837-0041-8, Jan. 2006, pp. 2-1 through 2-35.

13. Liu, Jiwen, Tam, C-J, Lu, T., and Law, C.K., "Simulations of Cavity-Stabilized Flames in Supersonic Flows Using Reduced Chemical Kinetic Mechanisms," AIAA Paper 2006-4862, 42nd AIAA Joint Propulsion Conf., 9-12 July 2006, 15 pp.

14. Humer, S., Frassoldati, A., Granata, S., Faravelli, T., Ranzi, E., Seiser, R., Seshadri, K., "Experimental and kinetic modeling study of combustion of JP-8, its surrogates and reference components," Proceedings of the Combustion Institute, **31** (2007), pp. 393-400.

15. Holley, A.T., Dong, Y., Andac, M.G., Egolfopoulos, F.N., Edwards, T., "Ignition and extinction of non-premixed flames of single-component liquid hydrocarbons, Jet fuels, and their surrogates," Proceedings of the Combustion Institute, **31**, 2007, pp. 1205-1213.

16. Allen, W., King, P.I., Gruber, M.R., Carter, C.D., and Hsu, K-Y, "Fuel-Air Injection Effects On Combustion In Cavity-Based Flameholders In a Supersonic Flow," AIAA Paper 2005-4105, 41st AIAA Joint Propulsion Conf., 10-13 July, 2005, 12 pp.

17. Lin, K-C, Tam, C-J, Boxx, I., Campbell, C, Jackson, K., and Lindsey, M., "Flame Characteristics and Fuel Entrainent Inside a Cavity flame Holder in a Scramjet Combustor," AIAA Paper 2007-5381, 43rd AIAA Joint Propulsion Conf., 8-12 July, 2007, 19 pp.

18. Lin, K-C, Jackson, K., Behdadnia, R., Jackson, T.A., Ma, F. Li, J., and Yang, V., "Acoustic Characterization of an Ethylene-Fueled Scramjet Combustor with a Recessed Cavity flameholder," AIAA Paper 2007-5382, 43rd AIAA Joint Propulsion Conf., 8-12 July, 2007, 11 pp.

19. Montgomery, C.J., Tang, Q., Sarofim, A.F., Bozzelli, J.W., "Supersonic Reacting Flow Simulations Using Reduced Chemical Kinetic Mechanisms and Multiprocessor ISAT," Paper AIAA 2008-1014, 46th AIAA Aerospace Sciences Meeting, 7-10 Jan., 2008, 10 pp.

20. Colket, M. Edwards, T, Williams, S, Cernansky, N.P., Miller, D.L., Egolfopoulos, F., Lindstedt, P., Seshadri, K., Dryer, F.L., Law, C.K., Friend, D, Lenert, D.B., Pitsch, H., Sarofim, A., Smooike, M., and

Tsang, W., “Development of an Experimental Database and Kinetic Models for Surrogate Jet Fuels,” Paper AIAA-2007-770, 45th AIAA Aerospace Sciences Meeting, 8-11 Jan., 2007, 21 pp.

21. Hongzhi, R. Zhang, Eddings, E. G., Sarofim, A.F., “Criteria for selection of components for surrogates of natural gas and transportation fuels,” Proceedings of the Combustion Institute, **31** (2007), pp. 401-409.

22. Valorani, M., Creta, F., Donato, F., Najm, H.N., Goussis, D.A., “Skeletal mechanism generation and analysis for *n*-heptane with CSP,” Proceedings of the Combustion Institute, **31** (2007), pp. 483-490.

23. Liu, S., Hewson, J.C., Chen, J.H., “Nonpremixed *n*-heptane autoignition in unsteady counterflow,” *Combust. Flame* **145**, (2006), pp. 730-739

24. Holley, A.T., Dong, Y., Andac, M.G., Egolfopoulos, F.N., “Extinction of premixed flames of practical liquid fuels: Experiments and simulations,” *Combust. Flame* **144**, (2006), pp. 448-460.

25. Andac, M.G. and Egolfopoulos, F.N., “Diffusion and kinetics effects on the ignition of premixed and non-premixed flames,” Proceedings of the Combustion Institute, **31** (2007), pp. 1165-1172.

26. Pellett, G.L., Isaac, K.M., Humphreys, W.M., Jr., Gartrell, L.R., Roberts, W.L., Dancey, C.L., and Northam, G.B., "Velocity and Thermal Structure, and Strain-Induced Extinction of 14 to 100% Hydrogen-Air Counterflow Diffusion Flames," *Combust. Flame* **112**, No. 4, 1998, pp. 575-592.

27. Pellett, G.L., Northam, G.B., Guerra, R., and Wilson, L.G., “Opposed Jet Burner Studies of Silane-Methane, Silane-Hydrogen, and Hydrogen Diffusion Flames with Air,” CPIA Publication 457, Vol. 1, Oct. 1986, pp. 391-404.

28. Pellett, G.L., Northam, G.B., Wilson, L.G., Jarrett, O., Jr., Antcliff, R.R., Dancey, C.L., and Wang, J.A., "Opposed Jet Diffusion Flames of Nitrogen-Diluted Hydrogen vs. Air: Axial LDA and CARS Surveys; Fuel/Air Strain Rates at Extinction," AIAA Paper 89-2522, July 1989, 19 pp.

29. Guerra, Rosemary, Pellett, G.L., Wilson, L.G., Northam, G.B., "Opposed Jet Burner Studies of Hydrogen Combustion with Pure and N_2, NO Contaminated Air," AIAA Paper 87-0090, Jan. 1987, 11 pp.

30. Guerra, Rosemary, Pellett, G.L., Wilson, L.G., Northam, G.B., "Opposed Jet Burner Studies of Effects of CO, CO_2 and N_2 Air Contaminants on Hydrogen-Air Diffusion Flames," AIAA Paper 87-1960, July 1987, 14 pp.

31. Pellett, G.L., Jentzen, M.E., Wilson, L.G., and Northam, G.B., "Effects of Water-Contaminated Air on Blowoff Limits of Opposed Jet Hydrogen-Air Diffusion Flames," AIAA Paper 88-3295, July 1988, 10 pp.

32. Pellett, G.L., Wilson, L.G., Northam, G.B., Guerra, Rosemary, "Effects of H_2O, CO_2, and N_2 Air Contaminants on Critical Airside Strain Rates for Extinction of Hydrogen–Air Counterflow Diffusion Flames," CPIA Publication 529, Vol. II, (Oct., 1989), pp. 23-42. Pasadena, CA, Oct., 1989.

33. Pellett, G.L., Northam, G.B., Wilson, L.G., "Counterflow Diffusion Flames of Hydrogen, and Hydrogen Plus Methane, Ethylene, Propane, and Silane, vs. Air: Strain Rates at Extinction," AIAA Paper 91-0370, Jan., 1991, 17 pp.

34. Pellett, G.L., Northam, G.B., Wilson, L.G., "Strain-Induced Extinction of Hydrogen–Air Counterflow Diffusion Flames: Effects of Steam, CO_2, N_2, and O_2 Additives to Air," AIAA Paper 92-0877, Jan., 1992, 15 pp. (Also an updated manuscript in preparation.)

35. Pellett, G. L., Roberts, W. L., Wilson, L. G., Humphreys, W. M., Jr., Bartram, S. M., Weinstein, L. M., and Isaac, K. M., "Structure of Hydrogen–Air Counterflow Diffusion Flames Obtained by Focusing Schlieren, Shadowgraph, PIV, Thermometry, and Computation,” AIAA Paper 94-2300, June 1994, 23 pp.

36. Pellett, G. L., Wilson, L. G., Humphreys, W. M.,Jr., Bartram, S. M., Gartrell, L. R., and Isaac, K. M., Roberts, W. L., IV, and Northam, G. B., "Velocity Fields of Axisymmetric Hydrogen-Air Counterflow Diffusion Flames from LDV, PIV, and Numerical Computation," AIAA paper 95-3112, July 1995, 23 pp.

37. Isaac, K. M., Ho, Y. H., Zhao, J., Pellett, G. L., and Northam, G. B., "Global Characteristics and Structure of Hydrogen-Air Counterflow Diffusion Flames: A One-Dimensional Model," AIAA Paper 94-0680, Jan.,1994. Also, Zhao, J., Isaac, K. M., and Pellett, G. L., *J. Propul. Power* **12**, No. 3 (1996), pp. 534-542.

38. Pellett, G.L., Isaac, K.M., and Nguyen, G., "Effect of Input Temperature on Strain-Induced Extinction of 50 to 100% Hydrogen–Air Counterflow Diffusion Flames," Presented at 27th Symposium (International) on Combustion, Abstracts of Work-In-Progress Poster Presentations, The Combustion Institute, Pittsburgh, PA, Poster W2D01, Aug., 1998, p. 192.

39. Pellett, G.L., Bruno, C., and Chinitz, W., "Review of Air Vitiation Effects on Scramjet Ignition and Flameholding Combustion Processes," AIAA Paper 2002-3880, July 2002, 37 pp.

40. Pellett, G.L., Bruno, C, and Chinitz, W., CHAPTER 4: Air Vitiation Effects on Scramjet Combustion Tests, in *Technologies for Propelled Hypersonic Flight*, RTO-TR-AVT-007, Volume 2 – Subgroup 4: Scram Propulsion, ISBNs 978-92-837-0041-4 / 978-92-837-0041-8, Jan. 2006, pp. 4-1 - 4-21.

41. Hwang, Kyu C., "Two Dimensional Numerical Simulation of Highly-Srained Hydrogen–Air Opposed Jet Laminar Diffusion Flames," Ph. D. Dissertation, Old Dominion University, Norfolk, VA, May 2003.

42. Convery, J.L., Pellett, G.L., O' Brien, W.F., and Wilson, L.G., "An Experimental Study of *n*-Heptane and JP-7 Extinction Limits in an Opposed Jet Burner," AIAA Paper 2005-3766, July 2005, 8 pp.

43. Convery, J.L., "An Experimental Investigation of JP-7 and *n*-Heptane Extinction Limits in an Opposed Jet Burner," MS Thesis in Mechanical Engineering, Virginia Polytechnic Institute and State University, Blacksburg, VA, October 27, 2005, 52 pp.

44. Pellett, G.L., Convery, J.L, Wilson, L.G., "Opposed Jet Burner Approach for Characterizing Flameholding Potentials of Hydrocarbon Scramjet Fuels," AIAA Paper 2006-5233, July 2006, 27 pp.

45. Pellett, G.L., Vaden, S.N., and Wilson, L.G., "Opposed Jet Burner Extinction Limits: Simple Mixed Hydrocarbon Scramjet Fuels vs Air," AIAA Paper 2007-5664, July 2007, 33 pp.

46. Pellett, G.L., Reid, Beth, McNamara, Clare, Johnson, Rachel, Kabaria, Amy, Panigrahi, Babita, and Wilson, L.G., "Acoustic Weakening of Methane-, Ethylene-, and Hydrogen-Air Counterflow Diffusion Flames, and Implications for Scramjet Flameholding." AIAA Paper 2003-4634, July 2003, 21 pp.

47. Pellett, G., Reid, B., McNamara, C., Johnson, R., Kabaria, A., Panigrahi, B., Sammons, K., and Wilson, L., "Dynamic Weakening of CH_4–, C_2H_6–, and C_2H_4/N_2–Air Counterflow Diffusion Flames using Acoustically Perturbed Inflows." Work-in-Progress Poster Paper 4F504, Presented at 30th International Symposium on Combustion, Abstracts of Work-In-Progress Posters, The Combustion Institute, Pittsburgh, PA, July 25-30, 2004.

48. Pellett, G.L., Kabaria, A., Panigrahi, B., Sammons, K., Convery, J., and Wilson, L.G., "Dynamic Weakening (Extinction) of Simple Hydrocarbon–Air Counterflow Diffusion Flames by Oscillatory Inflows." AIAA Paper 2005-4332, July 2005, 22 pp.

49. Pellett, G.L, McNamara, C., Johnson, R., Kabaria, A., Panigrahi, B., Sammons, K., Galgano, J., and Wilson, L.G., "Dynamic Weakening of Gaseous Hydrocarbon (C1-C4)–Air Counterflow Diffusion Flames by Oscillatory Inflows," Work-in-Progress Poster Paper 4B01, Presented at 31st International Symposium on Combustion, Abstracts of Work-In-Progress Poster Presentations, The Combustion Institute, Pittsburgh, PA, Aug. 6-11, 2006.

50. Spalding, D.B., "Theory of Mixing and Chemical Reaction in the Opposed-Jet Diffusion Flame," *J. Amer. Rocket Soc*., **3**, 1961, pp. 763-771.

51. Williams, F.A., "A Review of Flame Extinction," *Fire Safety J.*, **3**, 1981, pp. 163-175.

52. Guthhel, E., and Williams, F., **TITLE** 23rd *Symposium (International) on Combustion*, The Combustion Institute, Pittsburgh, 1990, p. 513.

53. Rolon, J.C., Veynante, D., Martin, J.P., and Durst, E., "Counter Jet Stagnation Flows," Experiments in Fluids, **11**, 1991, pp. 313-324.

54. Guthhel, E., Balakrishnan, G., and Williams, F., in *Reduced Kinetic Mechanisms for Application in Combustion Systems*, Lecture Notes in Physics (N. Peters and B. Rogg, eds.) Springer-Verlag, New York, 1992, p. 177.

55. Seiser, R., Truett, L., Trees, D., and Seshadri, K., "Structure and Extinction of Non-premixed *n*-Heptane Flames," 27th Symposium (International) on Combustion, The Combustion Institute (1998), pp. 649-657.

56. Hassan, M.I., Aung, K.T., Kwon, O.C., and Faeth, G.M., "Properties of Laminar Premixed Hydrocarbon / Air Flames at Various Pressures," *J. Propulsion and Power*, **14**, No. 4, 1998, pp. 479-488.

57. Bosschaart, K.J., and de Goey, L.P.H., "The Laminar Burning Velocity of Flames Propagating in Mixtures of Hydrocarbons and Air Measured with the Heat Flux Method," *Combustion and Flame*, **136**, 2004, pp. 261-269.

58. Ciani, Andrea, "Hydrogen and Methane Edge and Diffusion Flames in Opposed Jet Configurations: Structure and Stability." Dissertation, submitted to the Swiss Federal Institute of Technology Zurich, Switzerland, for the degree of Doctor of Technical Sciences, Doctoral Thesis ETH No. 16540, 2006, 108 pp.

59. Zambon, A.C, Chelliah, H.K., "Explicit reduced reaction models for ignition, flame propagation, and extinction of $C_2H_4/CH_4/H_2$ and air systems," *Combustion and Flame*, **150**, 2007, pp. 71-91.

60. Park, Okjoo, and Fisher, E.M., "Calculated extinction strain rates for binary fuel mixtures," Paper No. B-27, Eastern States Fall Technical Meeting of the Combustion Institute, U. of Virginia, Charlottesville, Va., Oct. 21-25, 2007.

61. Liu, Jiwen, Eklund, D., and Gruber, M., "Chemical Kinetic Mechanism Validation for Combustion of Mixture Fuel of Methane and Ethylene," Paper for presentation at the 55th JANNAF Propulsion Meeting, May 12-16, 2008, Boston, MA.

62. Dattarajan, S., Montgomery, C.J., Gouldin, F.C., Fisher, E.M., Bozzelli, J.W., "Extinction of Opposed Jet Diffusion Flames of Scramjet Fuel Components at Subatmospheric Pressures," AIAA Paper 2008-996, 46th AIAA Aerospace Sciences Meeting, 7-10 Jan, 2008, 9 pp.

63. Pellett, G.L., Vaden, S.N., Wilson, L.G., "Gaseous Surrogate Hydrocarbons for a HIFiRE Scramjet that Mimic Opposed Jet Extinction Limits for Cracked JP Fuels," Presented at 55th JANNAF Propulsion Meeting, 12-16 May, 2008, Boston, MA. JANNAF Paper-847 (2008), 38 pp.

64. Vaden, S.N., Debes, R.L., Lash, E.L., Burk, R.S., Boyd, C.M., Wilson, L.G., and Pellett, G.L., "Unsteady Extinction of Opposed Jet Ethylene / Methane HIFiRE Surrogate Fuel Mixtures vs. Air," AIAA paper 2009-4879, 45th AIAA/ASME/SAE/ASEE JPC, Aug, 2009, 22 pp.

65. Chinitz, W., and Erdos, J.I., "Test Facility Chemistry Effects on Hydrocarbon Flames and Detonations," AIAA Paper 95-2467, July 1995.

66. Fischer, K. and Rock, K, "Calculated Effects of Nitric Oxide Flow Contamination on Scramjet Performance," AIAA Paper 95-2524, July 1995, 12 pp. See also, Cabell, Karen F. and Rock, K.E., "A Finite Rate Chemical Analysis of Nitric Oxide Flow Contamination Effects on Scramjet Performance," NASA/TP-2003-212159, 33 pp.

67. Slack, M., and Grillo, A., "Investigation of Hydrogen-Air Ignition Sensitized by Nitric Oxide and by Nitrogen Dioxide," NASA CR-2896, 1977, 38 pp.

68. Laster, W.R. and Sojka, P.E., "Autoignition of H_2-Air: The Effect of NO_2 Addition," *J. Propulsion and Power*, **5**, No. 4, 1989, pp. 385-390.

69. Laster, W.R. and Sojka, P.E., "Autoignition of H_2/Air/NO_x Mixtures: The Effect of Temperature and Pressure," Technical Note, *J. Propulsion and Power*, **5**, No. 4, 1989, pp. 510-512.

70. Barannovskii, S.I., Nadvorskii, A.S., and Romashkova, D.D., (1989), "A Simple One-Dimensional Model of the Air Contamination Effect on Supersonic Combustion," *Comb., Detonation and Shockwaves*, Plenum Press, 1989, 24, pp. 677-685 (translation of *Fizika Goreniya i Vzryva*, 24, No. 6, pp. 42-51, 1988).

71. Zamansky, V.M., and Borisov, A.A., (1992), "Promotion of High Temperature Self-Ignition, " *Prog. Eng. Comb. Sci*., 18, 1992, pp. 297-325.

72. Ashmore, P.G., and Tyler, B.J., "The Nature and Cause of Ignition of Hydrogen and Oxygen Sensitized by Nitrogen Dioxide," *Ninth Symposium (International) on Combustion*, 1963, pp. 201-209.

73. Park, C., (1995), "Review of Finite-Rate Chemistry Models for Air Dissociation and Ionization," *Molecular Physics and Hypersonic Flow*, ed. by M.Capitelli, Kluwer Academic Publishers, Dordrecht, 1996.

74. Bulewicz, E.M. and Padley, P.J., *Thirteenth Symposium (International) on Combustion*, 1971, pp. 73-80.

75. Linteris, G.T., "Promotion of Hydrogen-Air Ignition by Iron Compounds," Paper No. C06, Fall Technical Meeting, Eastern States Section of the Combustion Institute, Oct. 21-24, 2007. 10 pp.

76. Mitani, T., "Ignition Problems in Scramjet Testing," *Combust. Flame*, **101**, 1995, pp. 347-349.

77. Mitani, T., (1994), "Effects of Dust from Storage Heaters on Ignition of Scramjets," NAL Technical Report TR-1234, 1994.

78. Candler, G.V., "Effect of Internal Energy Excitation on Supersonic Air Flow," AIAA Paper 99-4964, Nov. 1999, 9 pp.

79. Chelliah, H., "Intricacies of Counterflow Flames in Validating Chemical Kinetic Models," Presentation at 6th US National Combustion Conf., U. of Michigan, Ann Arbor, MI, May 2009.

80. Chelliah, H., "Intricacies of Counterflow Flames in Validating Chemical Kinetic Models," Paper presented at 2009 Fuels Summit, Sponsored by Multi-Agency Coordination Committee for Combustion Research (MACCCR), U. of Southern Cal., Los Angeles, Sept. 15-17, 2009, 25 pp.

81. Wang, Hai, et al., USC Mech II Optimized Chemical Kinetics Model, U. of Southern Cal., 2009.

82. Staff, Propulsion Chem. Div., Lewis Flt. Propulsion Lab, "Basic Considerations in the Combustion of Hydrocarbon Fuels with Air," NACA Report 1300, ed. by H.C. Barnett and R. R. Hibbard, 1959, 259 pp.

83. Dolvin, D.J., "Hypersonic International Flight Research and Experimentation," AIAA Paper 2009-7228, Oct. 2009, 11 pp.

APPENDIX A

The "original" 2008 Translation of Global ASR Extinction Limits

In the "original" translation [63], we first examined two slightly different empirical relationships between respective HC extinction limits for plug-inflow (7.2 mm nozzle based) and parabolic-inflow (7.56 mm tube-based) ASRs. This affected the subsequent scaling of respective global strain rates to axial strain rates *on an absolute basis* (note that comparable inflow strain rates were previously assessed independently using earlier PIV and Laser Doppler Velocimetry (LDV) with the same OJBs [26,35,36]). First, we tried a generalized linear fit of the data with a slope of 2.53 that related independent ASRs from nozzle-OJBs, ASR_n, to those from tube-OJBs, ASR_t. *However*, the fit had a significant intercept. Alternately, the same data were plotted with a forced zero intercept. Although this fit was not quite as good statistically, $ASR_n = 2.23\ ASR_t$ effectively characterized the absolute proportionality between plug-inflow and parabolic-inflow HC extinction results, and this simplified the data interpretation. Note the factor 2.23 also agreed very closely with a calculated average ASR ratio for *hydrocarbon*–air extinctions. Thus the 2.23 ASR ratio for HC–air CFDF extinctions was used to complete the conversion, as shown in the development of Eq. (2) below.

First it was important to examine three independent sources of relevant strain rate data [63]: (1) Rolon's detailed strain rate measurements of cold laminar "plug flows" of air vs air, using 25 mm diameter convergent nozzles; (2) our earlier PIV and LDV measurements of axial (and radial) strain rates, using 7.2 mm nozzle- and 7.5 mm tube-OJBs, that were consistent with plug inflow strain rates being ~ 2.5 x larger than parabolic inflow strain rates at the same average inflows [26,36]; and (3) Hwang's 2-D numerical simulations of opposed plug- and parabolic-inflows with equal mass flows [41] (see footnote[2]).

Thus, based on Rolon's and Hwang's results, we adopted a common "independently verified" proportionality (1.15) between the maximum axial strain rate input on the airside, $-(1/2)\ (du/dx)_{max}$, and the global ASR_n for a nozzle-OJB. In using the adopted value of 1.15, we can write (using the present nomenclature)

$$-(1/2)\ (du/dx)_{max} = 1.15\ ASR_n = \mathbf{1.15}\ U_{air}/D_n \qquad (1)$$

and then substitute the above-described experimentally demonstrated proportionality for gaseous HCs, $ASR_n = 2.23\ ASR_t$. By doing so, we define a globally based measure of maximum axial strain rate near the airside edge that can be used directly to compare experimental with computational results; i.e.:

$$-(du/dx)_{max} = \mathbf{2.30}\ U_{air}/D_n = 2.30 * 2.23\ U_{air}/D_t = \mathbf{5.13}\ U_{air}/D_t \qquad (2)$$

In comparison, note that Hwang's 2-D numerical simulations, using equal cold mass flows [41], defined the linear proportionality between opposed 5.0 mm nozzle (plug) inflows and tube (parabolic) inflows as $ASR_n = 2.53\ ASR_t$; and moreover the 2.53 applied not only for axial strain

[2] Hwang's 2-D numerical simulations of cold (300 K) plug and parabolic OJB impingement flows (with jet separation $H = D$) to determine respective axial and radial strain rates (velocity gradients) resulted in the following [41]: $-(1/2)\ (du/dx)_{max} = \mathbf{1.152}\ U_{air}/D_n$, and $(dv/dr)_{max} = \mathbf{1.158}\ U_{air}/D_n$ for **plug** inflows; and $-(1/2)\ (du/dx)_{max} = \mathbf{2.530} * 1.152\ U_{air}/D_t = \mathbf{2.91}\ U_{air}/D_t$; and $(dv/dr)_{max} = \mathbf{2.528} * 1.158\ U_{air}/D_t = \mathbf{2.93}\ U_{air}/D_t$ for **parabolic** inflows. Note that we previously deduced 3.0 (close to 2.91) from LDV and PIV surveys [26,35,36]. Thus -1/2 the maximum axial strain rate equals a common radial strain rate for *both* plug and parabolic inflows, and the respective axial and radial strain rates for plug inflows differ from the parabolic inflows by a ratio of **2.53**, which matches the slope of our cross-plotted data (2.53) and is quite close to the zero-intercept slope (2.23) obtained.

rates on the airside, but also for radial strain rates at the stagnation point. Perhaps coincidentally, the best fitting slope of our cross-plotted data was 2.53. Furthermore, for Hwang's numerically simulated H_2–air extinction "hot flows," the ratio of axial input strain rates for (equal mass flow rate) opposed 3.0 mm nozzle and 3.0 mm tube flows was very close to 2.5 [41], which is consistent with our PIV and LDV results [26,36].

The above-derived empirical expressions should quite accurately relate global ASRs, for laminar nozzle- and tube-OJB inflows, to maximum axial strain rate inputs near the airside edge of opposed cold and HC–air CFDFs. These should allow reasonably accurate comparisons of global experimental data with either numerically evaluated strain rates or measured maximum axial strain rates at extinction.

Fig. 9 reproduces our earlier direct comparison, on an *absolute* (local) airside maximum axial input strain rate basis, of our ASR extinction results for all the gaseous HCs studied in [63], with numerical strain rate results from Zambon & Chelliah [59], and Park & Fisher [60]. Before discussing the comparison, it is important to note how the experimental ASR results and numerical results were plotted on the absolute-strain-rate scales of the ordinate and the abscissa. The empirical Eq. (2) for airside axial strain rate (shown in Fig. 9 for the ordinate) enabled the plotting of all our experimental nozzle-OJB ASR_n results for gaseous HCs on the ordinate scale. The abscissa scale, which represents each experimental result for the respective gaseous HCs, was calculated from the expression on the abscissa label, which equals the second half of Eq. (2). In this way, the abscissa for each experimentally independent HC result could be calculated from the ASR_t data.

The numerical simulation results plotted on the ordinate scale simply represent calculated airside maximum axial strain rates. However, the abscissa for each numerical result corresponding to each HC is (of necessity) the same as that used to plot each experimental "tube-OJB airside axial strain rate." Therefore the vertical separation in Fig. 9 between numerical axial strain rate and experimental ASR_n results represents an absolute discrepancy in airside maximum axial strain rate for each gas or gas mixture.

Finally, inspection of the "original" Fig. 9 indicates there was exceptionally good agreement between Zambron and Chelliah's methane extinction limit at 1 atm with our experimentally averaged result; this "baseline result" was checked and reproduced repeatedly and semi-independently over the last 10 years [26]. Additional agreement with Ref. 61 numerical results for methane (not shown), using three recent kinetic models, appeared to be similarly good. However, the numerical ethylene results from Refs. 59 and 60 were about 45 % higher than the experimental result for ethylene, and the Ref. 61 numerical results were respectively about 50 %, 40 %, and 30 % high of the experimental result for ethylene. Due to the near-linear divergence of results from the methane "base," predicted results for the 64 % ethylene + 36 % methane surrogate also appeared to be about 45 % high. Finally, the results of Park and Fisher [60] and Jiwen Liu [61] independently predicted the observed experimental nonlinear FS response as a function of ethylene concentration.

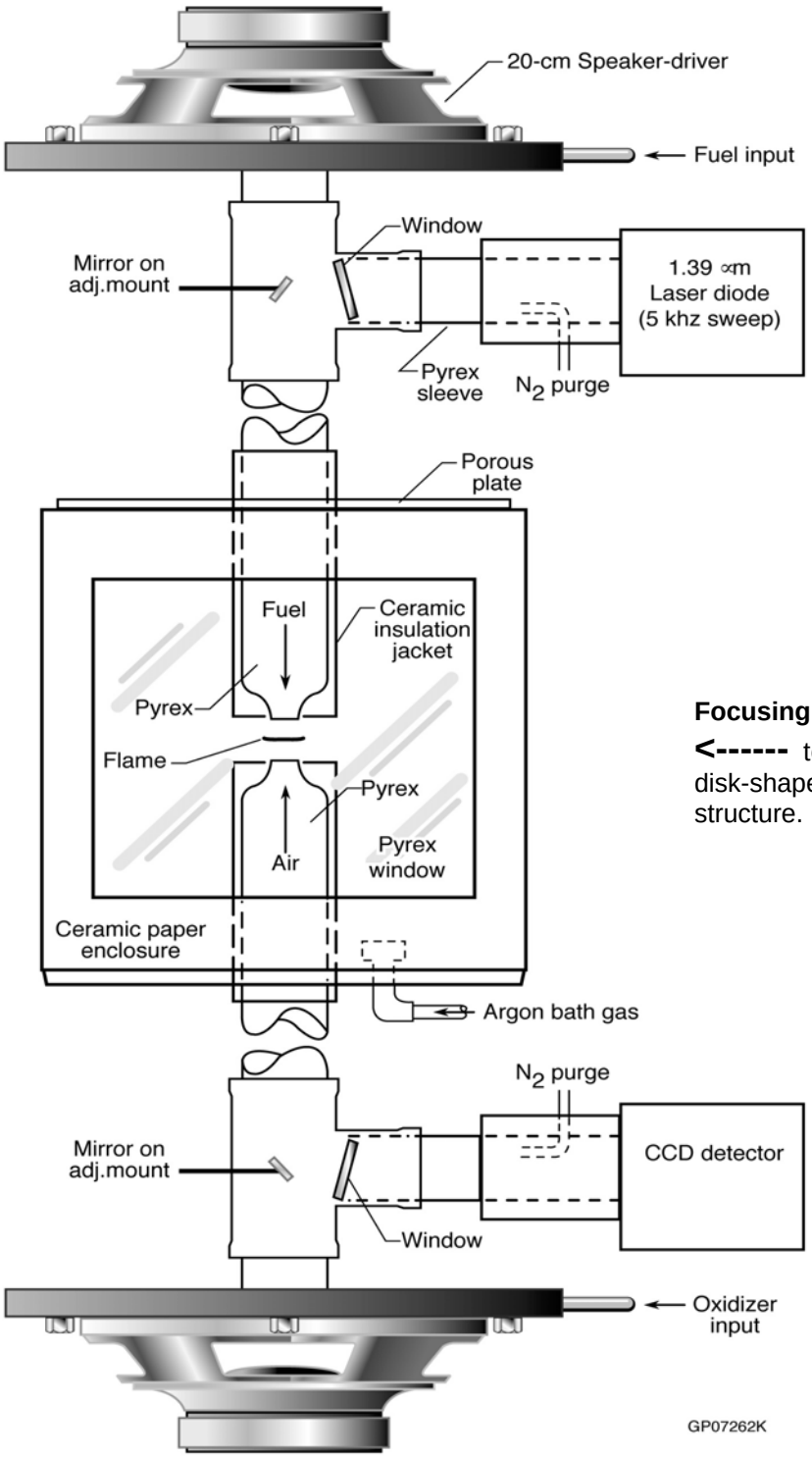

Focusing Schlieren System used continuously

<------ to visualize flows, including centering of disk-shaped flame, and vertical / horizontal structure. Details in [26,35,36]

Fig. 1a. Schematic of the Oscillatory Opposed Jet Burner (OOJB) system with twin 20-cm speaker-drivers, used to determine both steady-state FS and Dynamic Flame Weakening. Diode laser system is passive in this study.

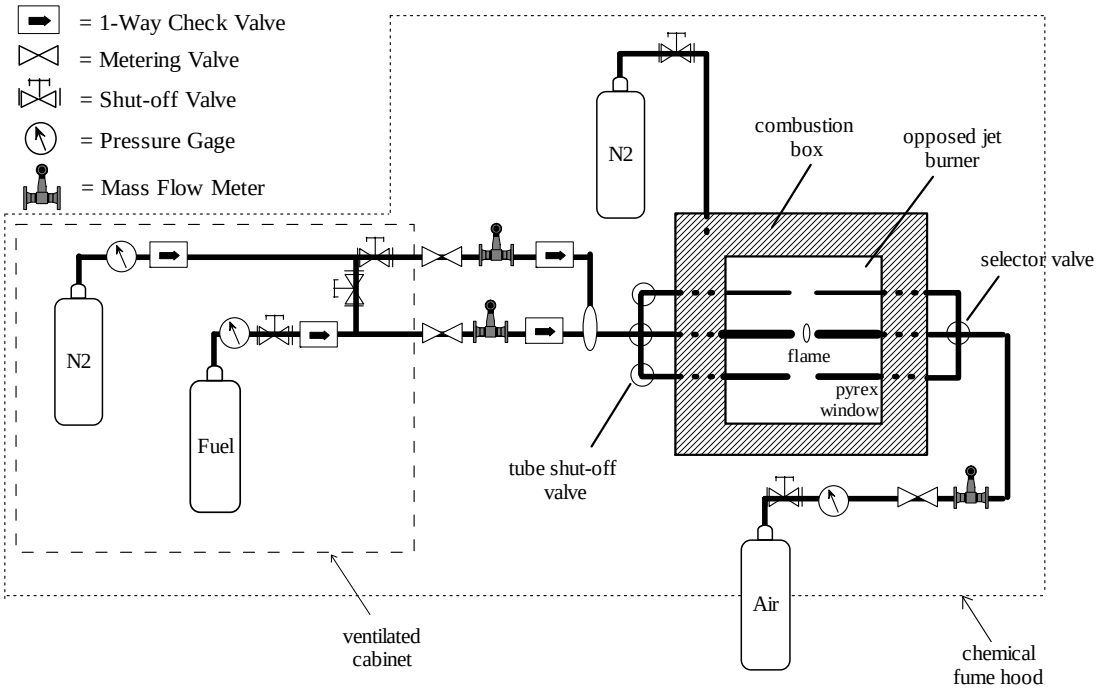

Fig. 1b. Gaseous-fuel horizontal-tube OJB test schematic (not to scale). Combustion box, constructed of 0.5 in thick compacted silica fiber-board panels, has a porous metal plate on top -- typically 4 x 6 in -- is exposed and "active". Thus combustion products are actively purged by controlled nitrogen flows from two porous plug outlets at opposite corners of the box floor. The three matching sets of tube-OJBs are actually arrayed in a horizontal plane, not vertically as shown. Mass flows of fuel, fuel-diluent, air, and air contaminant are monitored as flame extinction and restoration limits are approached and achieved.

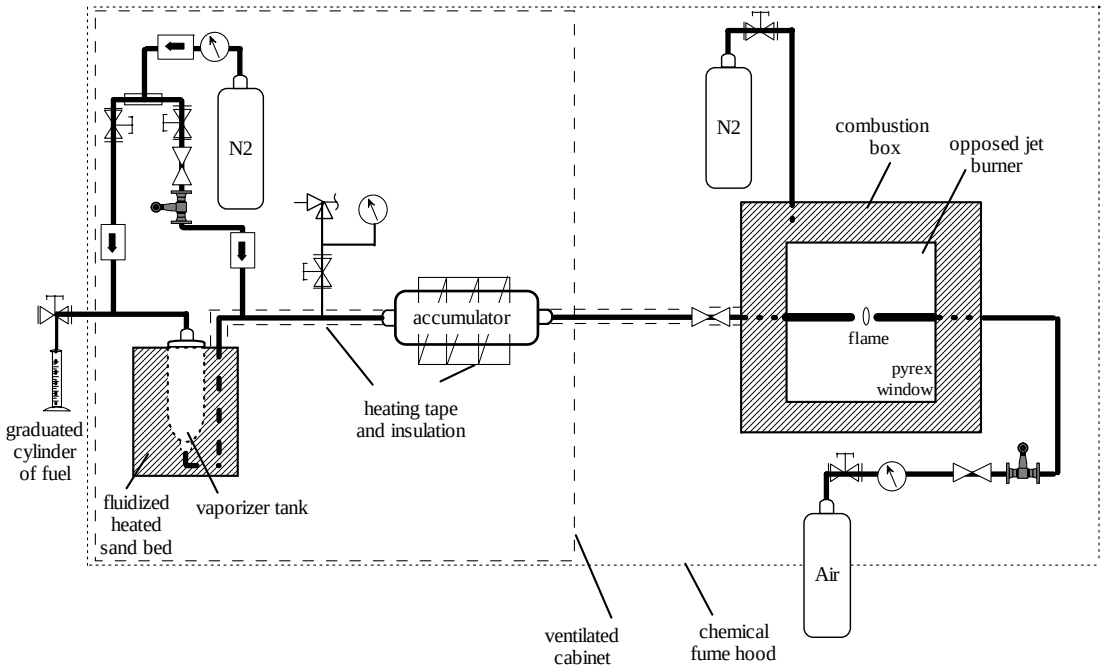

Fig. 1c. Complete HC-fueled OJB test schematic (not to scale). Silica fiber combustion box, with porous plate on top, is identical to that in Fig. 1b. Vaporizer tank is ~ 0.5 L and accumulator tank is ~ 10.1 L. For batch tests, a known volume of liquid HC is injected into the cold, evacuated system. Then mass-flow-metered fuel diluent (either N_2 or gaseous HC) is admitted, up to a specific pressure. Finally, the system is sealed and heated to a measured (multipoint) temperature and pressure, and held there to assure mixing before operating in a "blow down mode," to supply the 7.5 mm tube-OJB system. For hot vaporized-fuel experiments, air mass flows are monitored, but mass flows of fuel mixture are not monitored due to temperature limitations. For tests with gaseous fuels the vaporizer-accumulator is bypassed and mass flows of all fuel and components are measured.

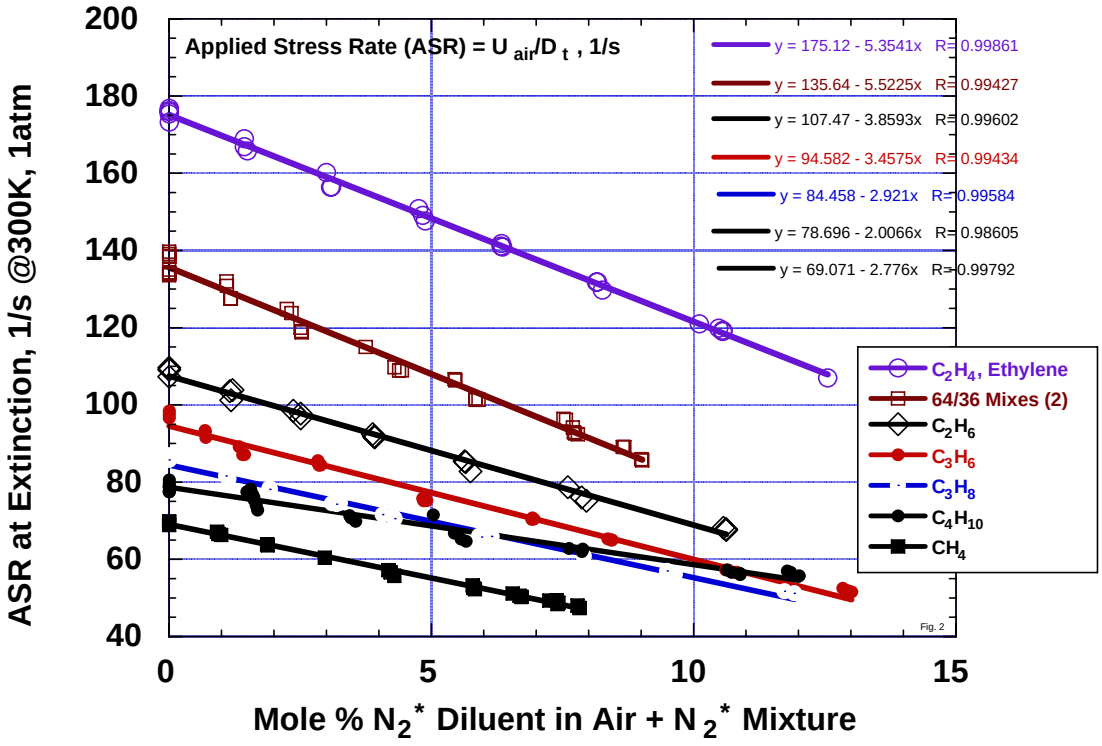

Fig. 2. Effects of N_2* dilution (contamination) of clean dry air on ARS at extinction of HC vs. air Counter Flow Diffusion Flames (CFDFs), using 9.3 mm Tube-OJB system at 1-atm. The "64/36" surrogate fuel mixture data are combined from independent measurements, from the two premixed bottles used for testing in the Arc-Heated Scramjet Test Facility (AHSTF).

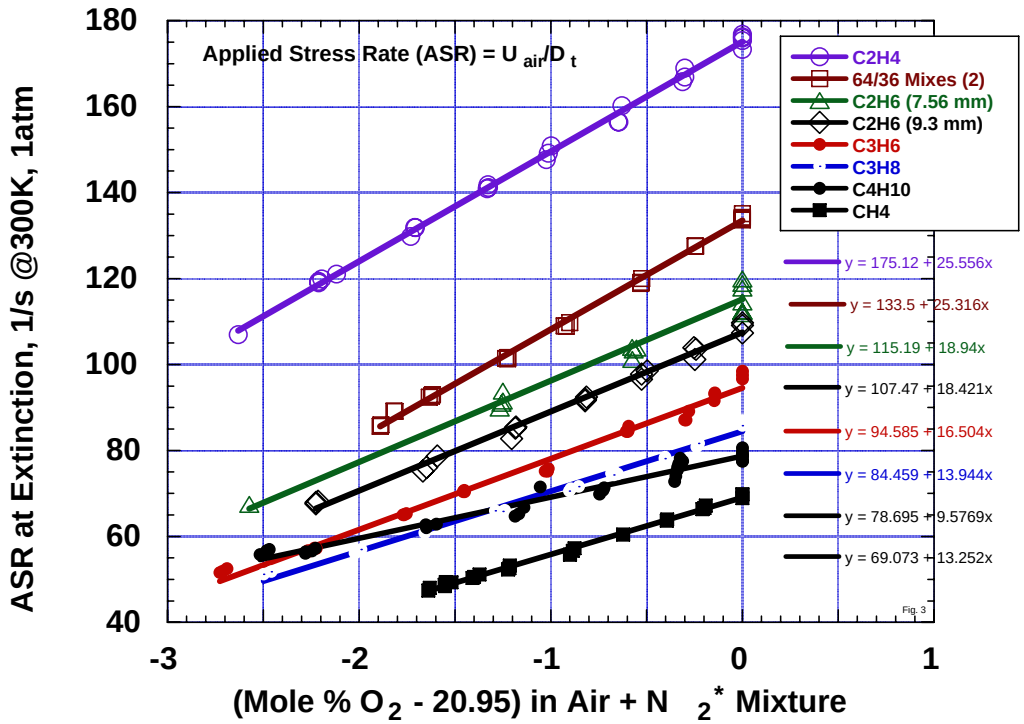

Fig. 3. Effects of mole % O_2 in N_2* contaminated air on extinction of HC vs. Air CFDFs, using 9.3 (and 7.56 mm for C_2H_6) tube-OJB system at 1-atm. The 9.3 mm data are the same as plotted in Fig. 2.

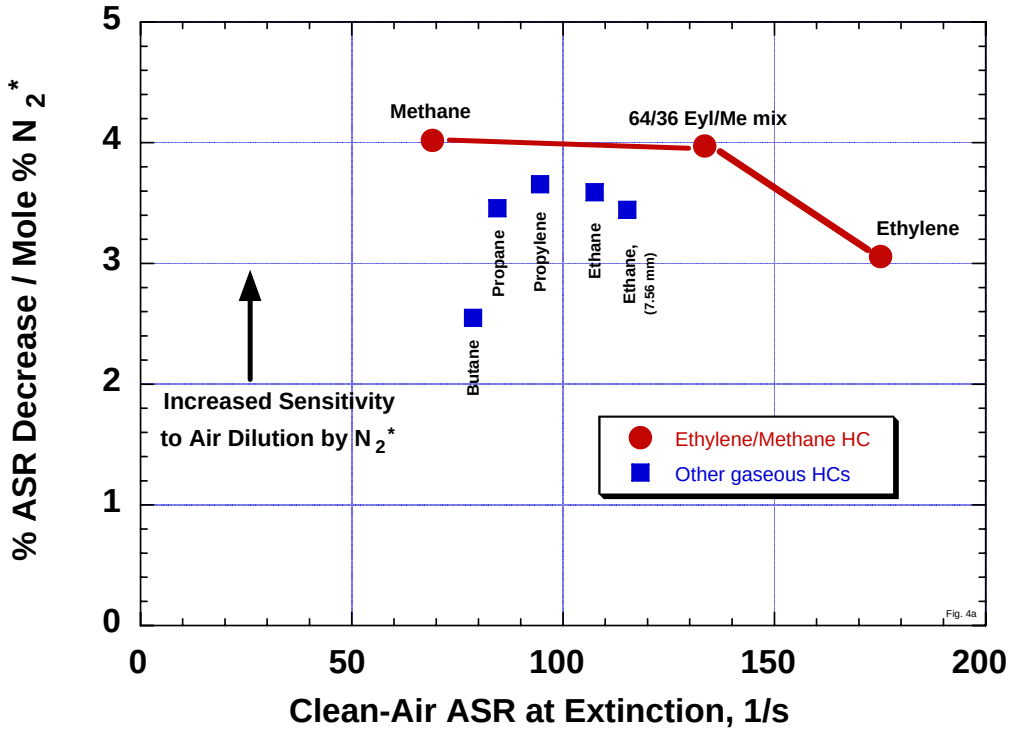

Fig. 4a. Sensitivity of ASR at extinction to mole % N_2* added to air, which decreased O_2 content in contaminated airs for various HC vs. "air" CFDFs, using 9.3 mm tube OJB system at 1-atm. Results were obtained by normalizing the respective slopes with intercepts from Fig. 2.

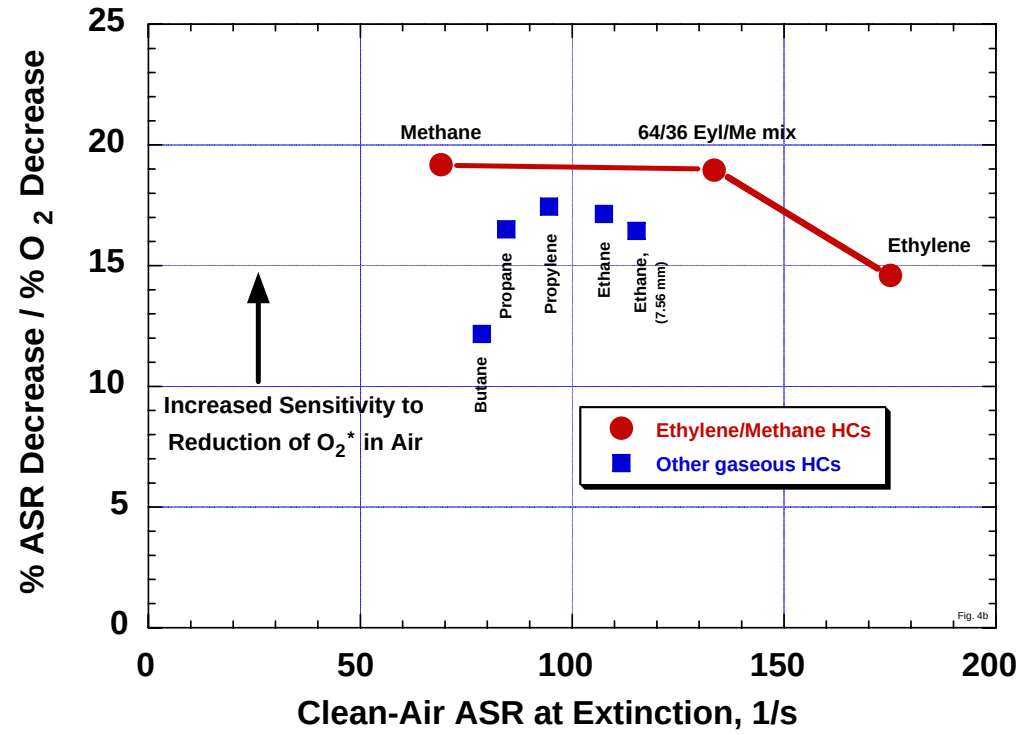

Fig. 4b. Sensitivity of ASR at extinction to mole % O_2 decrease in N_2* diluted air, for various HCs vs. "air", using 9.3 mm tube OJB system at 1-atm. Results were obtained by normalizing the respective slopes with intercepts from Fig. 3.

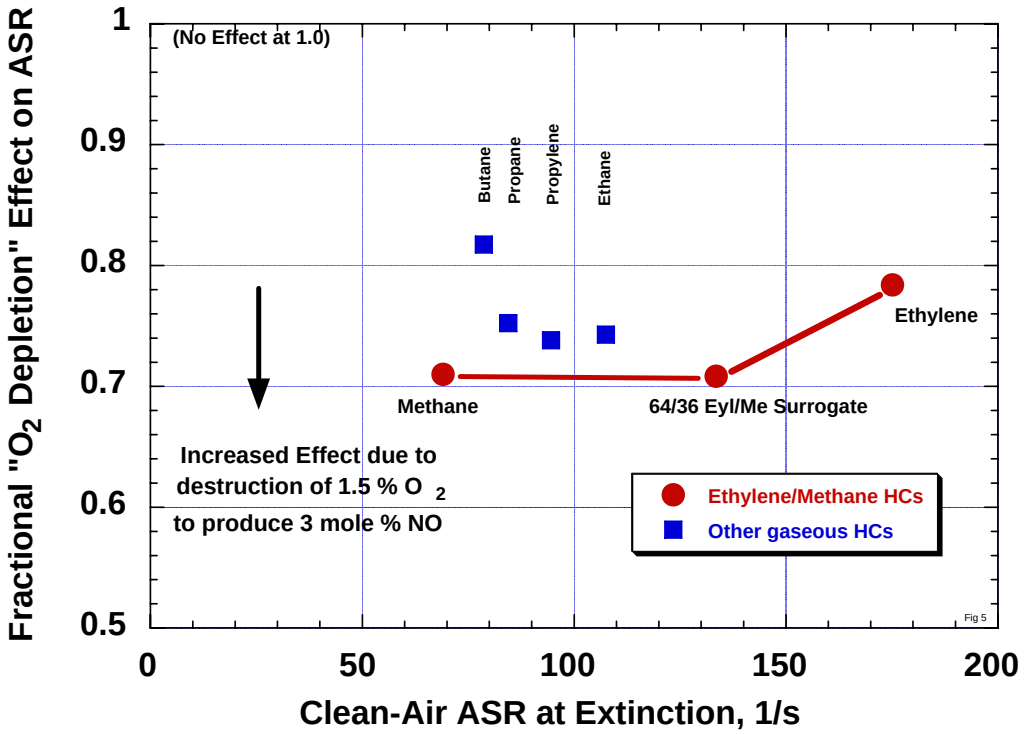

Fig. 5. Fractional "O_2 depletion" effect on ASR at extinction, due to consumption of 1.5 mole % O_2 and 1.5 mole % N_2 in Arc-Heated air to produce 3 % NO, for various HC vs. air systems, using 9.3 mm tube-OJB at 1-atm. Fractional "O_2 depletions" were obtained from linear curve fits of the Fig. 3 data.

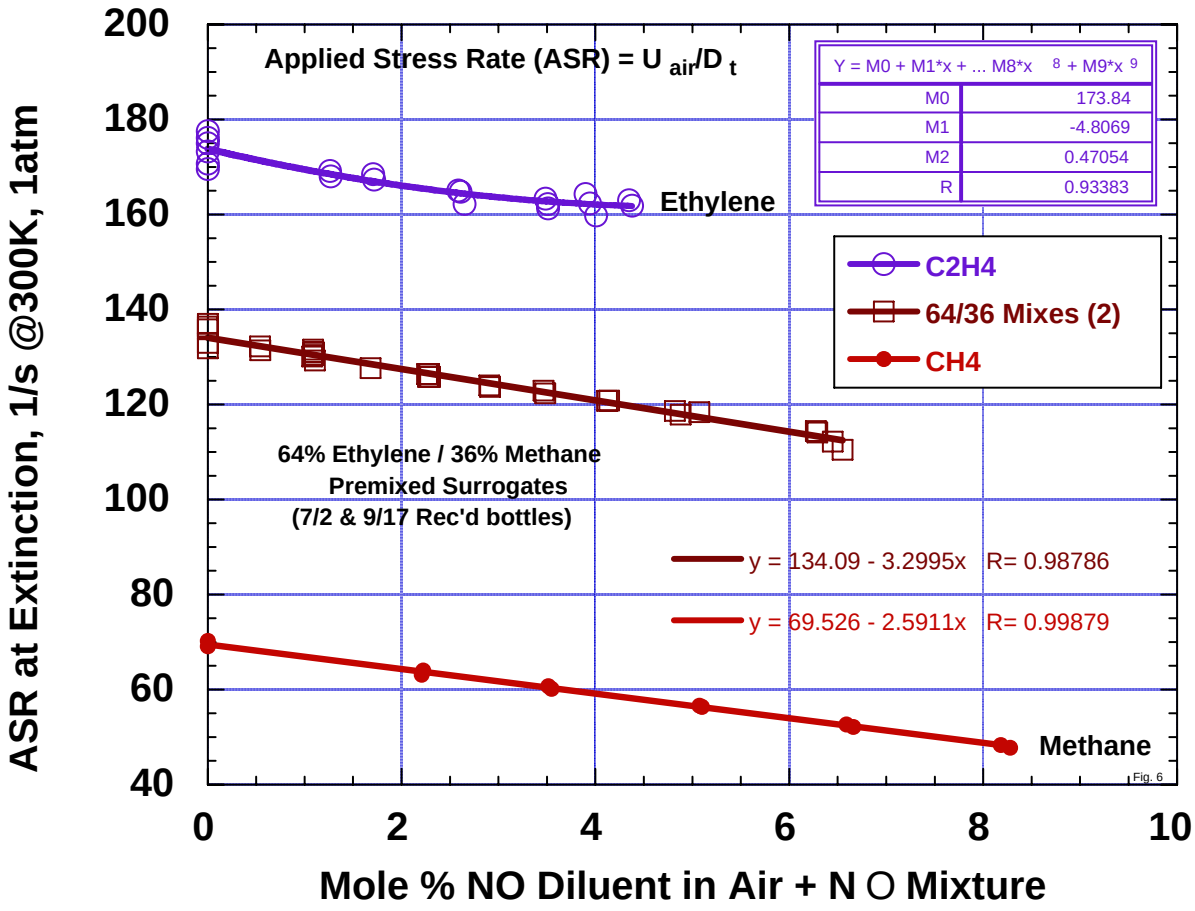

Fig. 6. Effects of NO dilution (contamination) of air on extinction of HCs vs. air DFDFs, using 9.3 mm tube-OJB system at 1-atm. The experimental system and procedure were identical to that used in obtaining the Fig. 2 results. The "64/36" surrogate fuel mixture data are combined from independent measurements, from the two premixed bottles used for testing in the AHSTF.

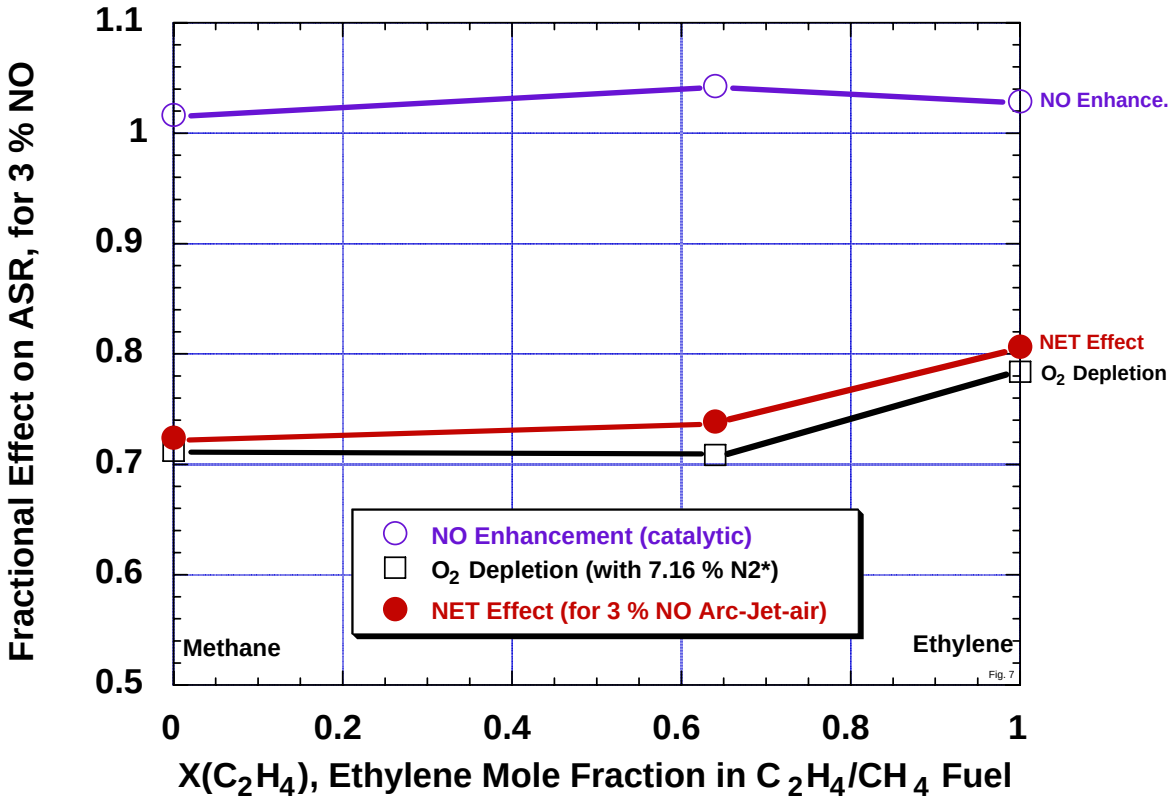

Fig. 7. Fractional effects on ASR at extinction, for HC vs. simulated Arc-Heated air with 3 mole % NO, for respective "NO enhancement", "oxygen depletion" and "net" effects on ASR, based on 9.3 mm tube-OJB results at 1-atm. Note that use of 'an effective' 7.16 % N_2* diluted air from the OJB results is required to produce the correct O_2 concentration for 3 % NO in simulated Arc-Heated air with a resultant 19.45 % O_2 (from 20.95 % O_2 in the original dry air).

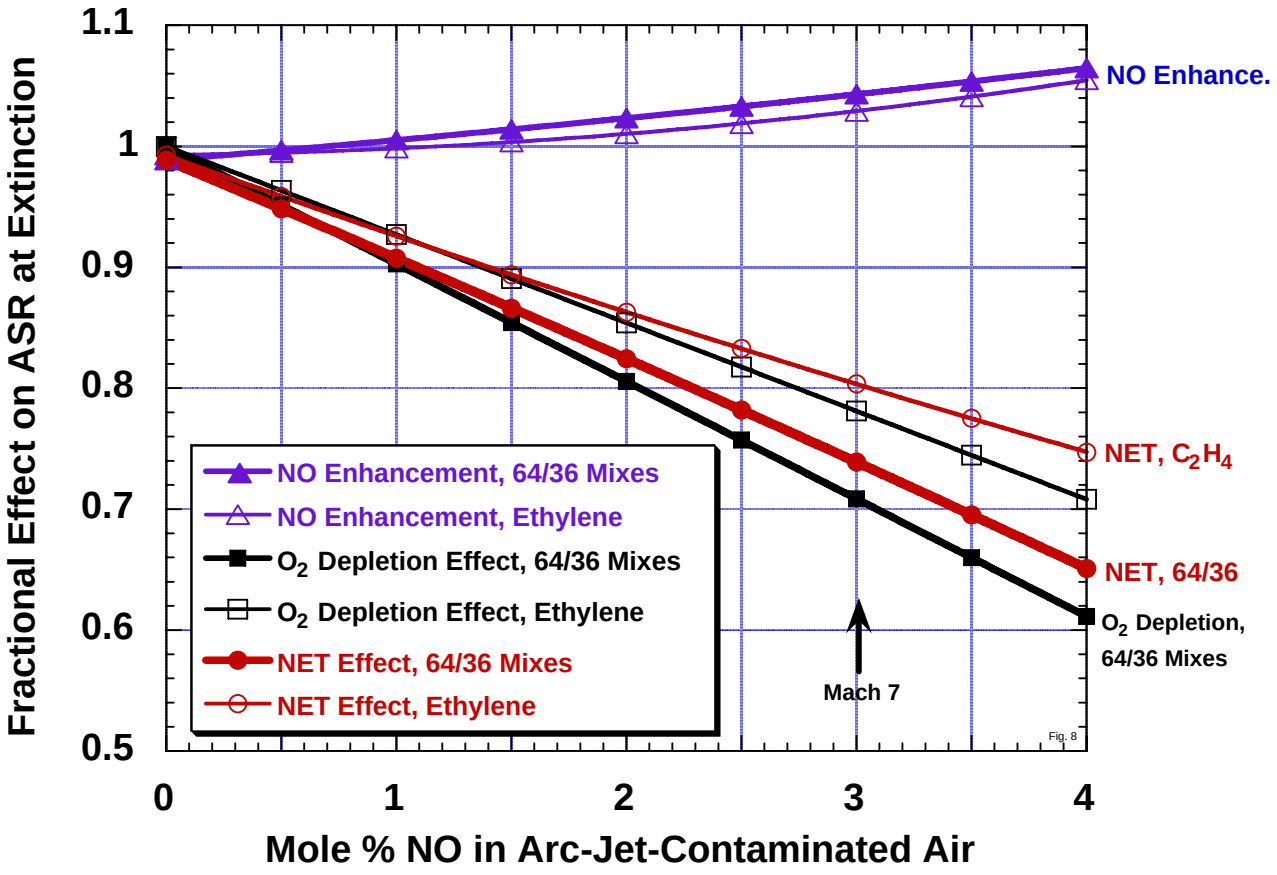

Fig. 8. Projected fractional effects on ASR at extinction, for ethylene and the "64/36" surrogate mix vs. simulated Arc-Heated contaminated air, for "NO enhancement", "oxygen depletion" and "net" effects, from 9.3 mm tube-OJB results at 1-atm. The 3 % NO corresponds approximately to a free stream Mach number of 7.

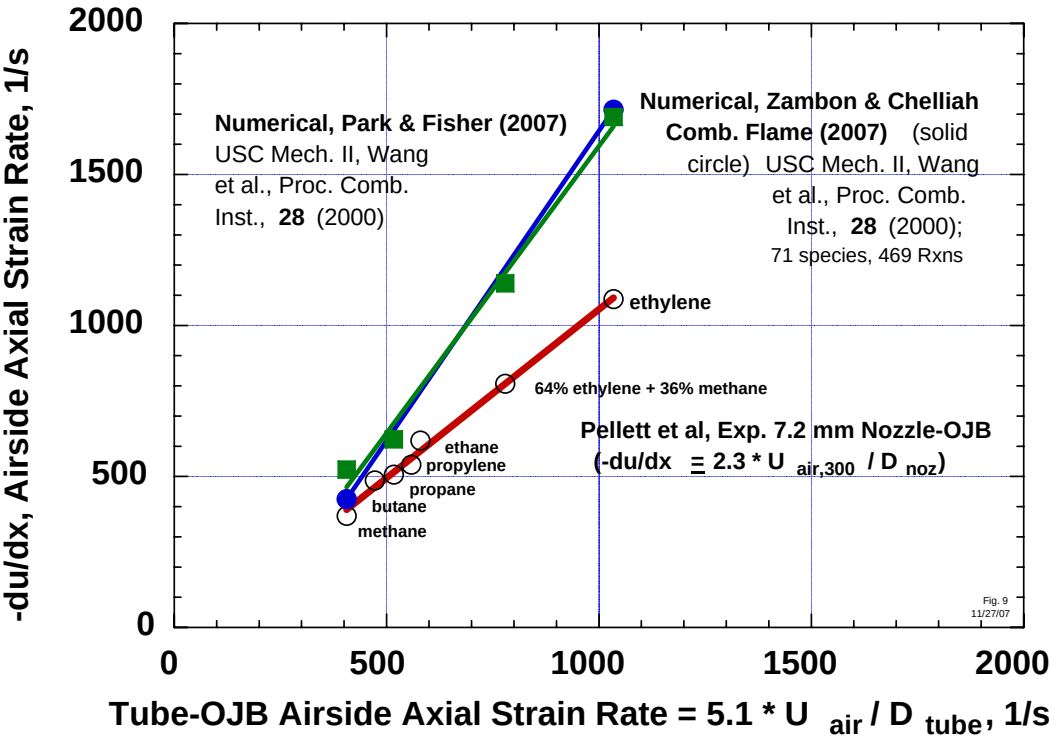

Fig. 9. Previously presented [63] comparison of experimental and numerically simulated strain induced extinction limits for Fuel vs Air CFDFs at 1 atm, using best-estimate global measures of (local) airside maximum axial strain rates (see development in text and in Appendix A.)

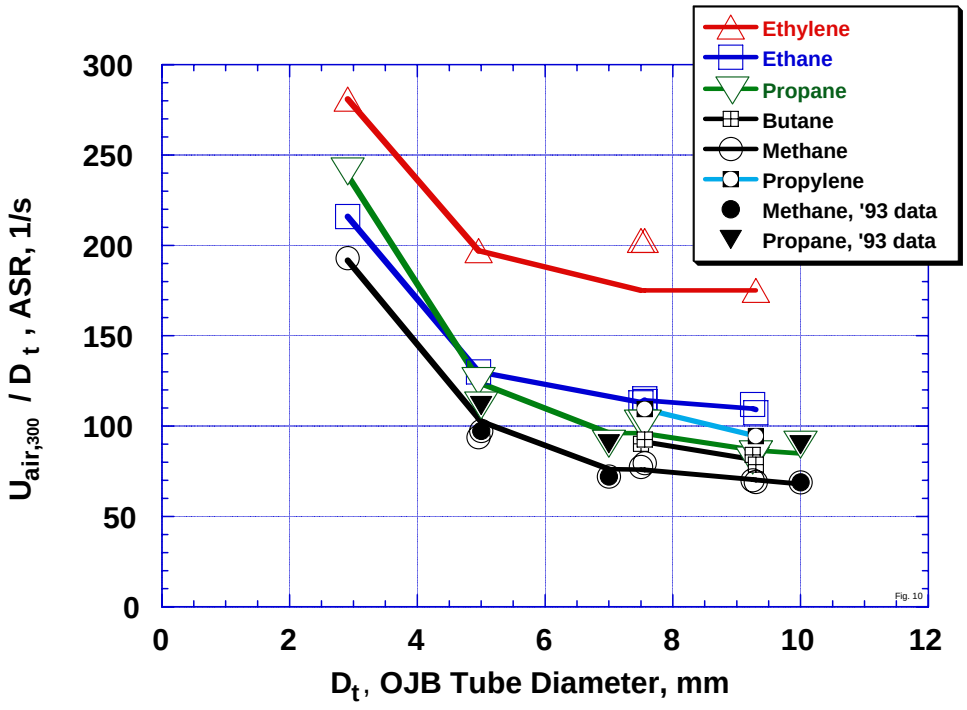

Fig. 10. Effect of OJB straight-tube diameter on Applied Stress Rate, ASR = U_{air} / D_t , for various gaseous HCs vs. air CFDF systems investigated over the last 20 years, including the present 9.3 mm results. Asymptotic approach characterizes the diminishing effects of finite flame thickness and finite OJB size that are limited by the requirement of lamainar flows.

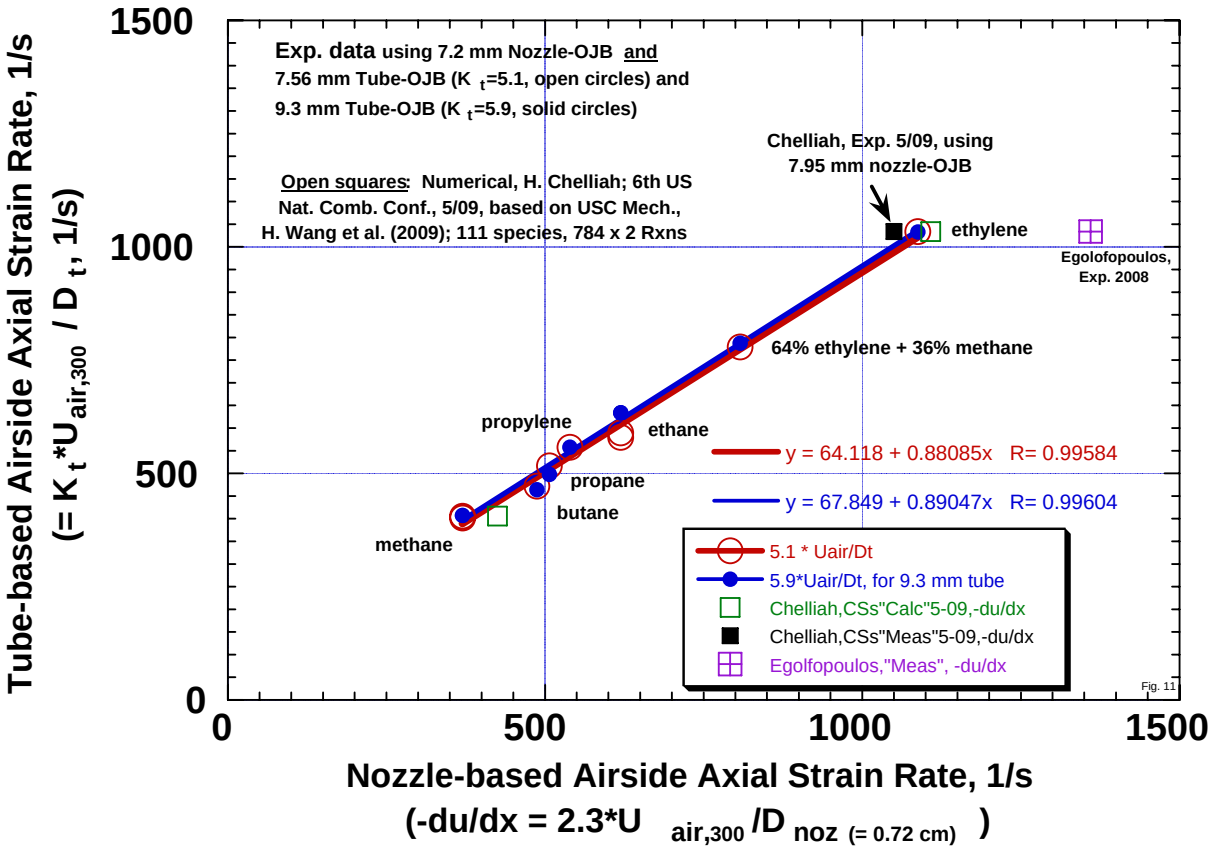

Fig. 11. Comparison of experimental and numerical strain-induced extinction limits for pure fuel vs. air Counterflow Diffusion Flames at 1-atm, using best estimates (based on measurements) of (local) airside axial strain rate. Note the present $\pm$ 5 % agreement for ethylene based on four independent results from NASA Larc and UVa. The open circles represent the same 2008 (and earlier) OJB data shown in Fig. 9; the solid circles represent the new 9.3 mm data; the solid square represents H. Chelliah's new experimental data (UVa) [79,80]; and the open square represents H. Chelliah's numerically obtained extinction limit (UVa) [79,80] obtained using Hai Wang's newly updated (2009) chemical kinetic model (USC) [81].

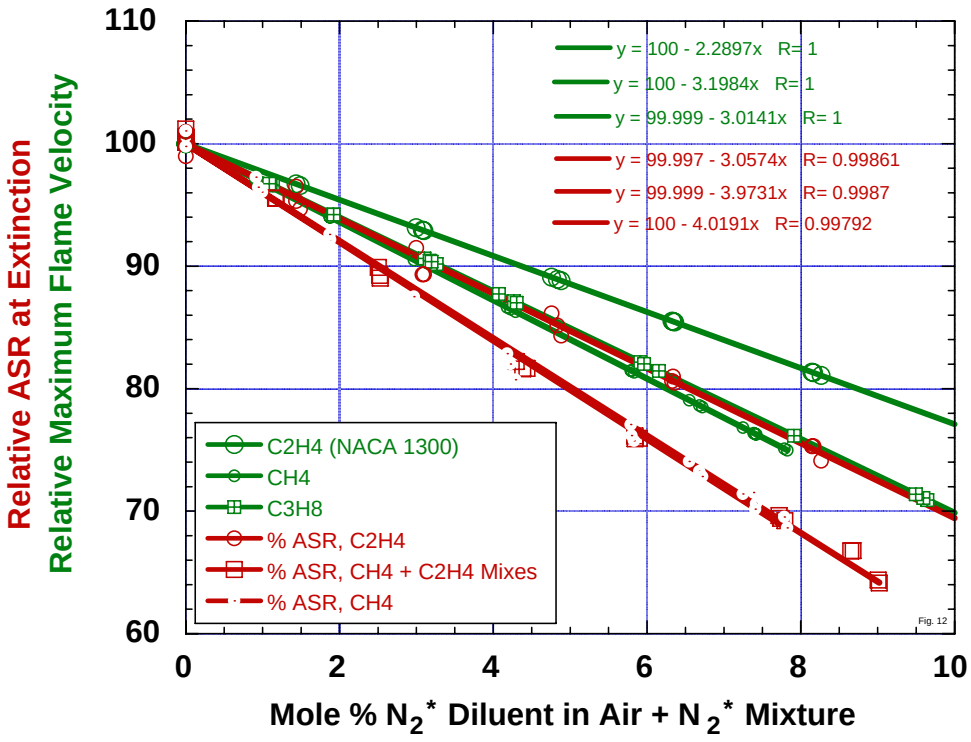

Fig. 12. Relative effects of N_2* dilution of air ("oxygen dilution" effect) on extinction of HC vs. contaminated-air CFDFs, using 9.3 mm tube-OJB at 1-atm; and comparison with relative "maximum flame speed" for premixed HC + O_2 + N_2 systems reported in [82]. Recall that addition of 7.16 mole % N_2* to clean air is required in using OJB extinction results to simulate the resultant O_2 content (19.45 %) in an Arc-Heated contaminated air containing 3 mole % NO.